Characterization of Caveolin-1 as a Modulator of Airway Smooth Muscle Responsiveness *ex vivo* and *in vivo*

By

Sarah Maltby

A thesis submitted to the Faculty of Graduate Studies of

The University of Manitoba

In partial fulfillment of the requirements of the degree of

Master of Science

Department of Physiology

University of Manitoba

Winnipeg

Acknowledgements

I would like to extend my sincere gratitude to my supervisor, Dr. Andrew Halayko, whose knowledge and enthusiasm have been invaluable in the completion of this project. I am extremely grateful that he has been so patient while I was writing and attending medical school. I would especially like to thank Sujata Basu for teaching me the technical skills required to complete this research and for her constant help and support. I would also like to acknowledge all the members of the Halayko lab, especially Dr. Reinoud Gosens and Dr. Dedmer Schaafsma, for their assistance and advice throughout my research project.

Being a member of The Biology of Breathing Research Theme and the National Training Program in Allergy and Asthma was extremely helpful and important. The members of both teams were always willing to answer my questions and share their opinions. I wish to express my sincere gratitude to them for providing an interactive research environment. I would also like to thank my committee members, Dr. Fedirchuk, Dr. Soussi-Gounni and Dr. Kroeger for challenging my knowledge of medical physiology and helping me to identify my strengths and weaknesses. It has made me a more competent researcher. Finally, I would like to thank the Manitoba Institute of Child Health at the John Buhler Research Centre for the use of their facility and equipment.

Table of Contents

Acknowledgements....2

List of Figures....5

List of Tables....6

List of Abbreviations....7

I. Abstract....9

II. Objectives and Rationale....11

III. Literature Review....13

Asthma....13

Characteristic Features of Asthma....13

Asthma Pathogenesis....15

Allergic Sensitization....15

The Epithelial-Mesenchymal Trophic Unit & Airway Remodeling...17

Caveolae & The Caveolin Gene Family....19

Caveolin-1 Knockout Mice....21

Caveolae in Human Disease....22

Caveolin-1 & Fibrosis....23

Smooth Muscle Contraction....25

Caveolae & Smooth Muscle Contraction....28

Caveolin-1 & Inflammation....31

IV. Hypothesis and Specific Aims....32

V. Materials and Methods.....34

VI. Results.....45

VII. Discussion.....69

VIII. References.....79

List of Figures

Figure 1: Structure and functional domains of caveolae……20

Figure 2: Calcium-dependent mechanism of smooth muscle contraction……26

Figure 3: Calcium-independent mechanisms of smooth muscle contraction……28

Figure 4: Expression of caveolins in isolated tissue from caveolin-1 knockout mice and B6129SF2/J mice……45

Figure 5: Electron micrograph of airway smooth muscle cells from the central airways of caveolin-1 knockout mice and B6129SF2/J mice……46

Figure 6: Respiratory mechanics of caveolin-1 knockout, B6129SF2/J and C57BL/6 mice……48

Figure 7: Comparison of collagen abundance in large, medium and small airways in caveolin-1 knockout and B6129SF2/J mice……52

Figure 8: Comparison of airway smooth muscle α-actin abundance in large, medium and small airways in caveolin-1 knockout and B6129SF2/J mice……53

Figure 9: Comparison of the baseline inflammatory profile between caveolin-1 knockout mice and B6129SF2/J mice……55

Figure 10: Assessment of airway (tracheal) smooth muscle contraction via myography……58

Figure 11: Effect of protein kinase C (PKC) inhibition on methacholine induced tracheal smooth muscle contraction……61

Figure 12: Effect of extracellular signal related kinase (ERK1/2) inhibition on methacholine induced tracheal smooth muscle contraction……62

Figure 13: Effect of RhoA/Rho kinase (ROCK1/2) inhibition on methacholine induced tracheal smooth muscle contraction……65

Figure 14: Respiratory mechanics of caveolin-1 knockout (Cav-$1^{-/-}$) and B6129SF2/J following inhalation of RhoA/Rho kinase (ROCK1/2) inhibitor, Y-27632……67

Figure 15: Abundance of RhoA, ROCK 1, and ROCK 2 protein expression in lung and trachea tissue from caveolin-1 knockout (Cav-$1^{-/-}$) and B6129SF2/J mice……68

List of Tables

Table 1: Average basement membrane length of airways from caveolin-1 knockout (Cav-$1^{-/-}$) and B6129SF2/J mice……49

Table 2: Contractile properties of tracheal preparations obtained from B6129SF2/J and caveolin-1 knockout (Cav-$1^{-/-}$) mice.....60

List of Abbreviations

ACh: Acetylcholine

AHR: Airway hyperresponsiveness

AP-1: Activator protein 1

BALF: Bronchoalveolar lavage fluid

B6129SF2/J: Wild type controls for caveolin-1 knockout mice

$[Ca^{2+}]_i$: Intracellular calcium concentration

Cav: Caveolin

Cav-1: Caveolin – 1

Cav-$1^{-/-}$: Caveolin – 1 knockout mice

c-Src: Cellular-src family tyrosine kinase

DAG : Diacylglycerol

ECM: Extracellular matrix

eNOS: Endothelial nitric oxide synthase

ERK1/2: Extracellular signal regulated kinase 1/2

G: Tissue resistance

GEF: Guanine nucleotide exchange factors

IgE: Immunoglobulin E

IL- : Interleukin -

IFN-γ: Interferon gamma

IP3: Inositol triphosphate

IPF: Interstitial pulmonary fibrosis

LPS: Lipopolysaccharide

MAPK: MKK3/p38 mitogen activated protein kinase

MLC_{20}: Myosin light chain

MLCK: Myosin light chain kinase

MLCP: Myosin light chain phosphatase

MYPT1: Myosin phosphatase targeting subunit

NF-κB: Nuclear factor κ B

NO: Nitric oxide

PKC: Protein kinase C

PLC: Phospholipase C

PP1c: Catalytic subunit of myosin light chain phosphatase

Rn: Central airway resistance

ROCK1/2: Rho kinase

siRNA: Small interfering ribonucleic acid

SR: Sarcoplasmic reticulum

TGF-β1: Transforming growth factor beta

TNF-α: Tumour necrosis factor alpha

I. Abstract

Caveolin-1 (Cav-1) is a marker protein for caveolae and can be a regulator of intracellular signaling pathways. It has been implicated in human cancer, cardiovascular disease and idiopathic pulmonary fibrosis. In the present study, the structural and functional changes of the lung in Cav-1 null mice (Cav-$1^{-/-}$) were assessed. Respiratory mechanics, measured using a small animal ventilator, revealed heightened methacholine-induced maximum central airway resistance (Rn) and tissue resistance (G) as well as enhanced tissue elastance (H). Morphometric analyses revealed respiratory hyperreactivity is associated with increased collagen deposition around central and peripheral airways in Cav-$1^{-/-}$ mice. However, compared to control (B6129SF2/J) mice, smooth muscle α-actin staining of contractile tissue mass was unchanged in peripheral airways and was marginally reduced in central airways. To assess functional status of airway smooth muscle, we measured methacholine concentration-response characteristics of tracheal rings mounted on an isometric wire myograph. Similar to that observed for Rn *in vivo*, compared to controls, tracheal preparations from Cav-$1^{-/-}$ mice exhibited a significant increase in maximum active contractile force without a change in sensitivity (EC50). Rho kinase (ROCK1/2), protein kinase C (PKC) and extracellular signal regulated kinase 1/2 (ERK1/2) signaling were assessed as possible sources of the enhanced airway reactivity observed in Cav-$1^{-/-}$ mice. Aerosol pre-exposure of both Cav-$1^{-/-}$ and B6129SF2/J to Y-27632, a potent Rho kinase inhibitor, markedly blunted *in vivo* lung function responses (Rn) and G) to inhaled methacholine and eliminated differences between strains. Moreover, pretreatment with Y-27632 (10μM) reduced the sensitivity and maximum response to methacholine in tracheal ring preparations from both Cav-$1^{-/-}$ and B6129SF2/J, completely normalizing the difference in contractile responses that exist between mouse strains. Notably, though pretreatment with the PKC inhibitor

GF 109203X and the ERK1/2 inhibitor U0126 moderately suppressed methacholine-induced contractile force, the effect was of equal magnitude on Cav-$1^{-/-}$ and B6129SF2/J mice. In addition, we measured basal airway inflammation in Cav-$1^{-/-}$ mice using bronchoalveolar lavage fluid (BALF). Total inflammatory cell number, the differential abundance of eosinophils, neutrophils, lymphocytes, and macrophages, and the abundance of Th1 and Th2 cytokines (IL-5 and IFN-γ) were comparable between Cav-$1^{-/-}$ and control mice. In contrast, TGF-β1 and TNF-α were fourfold higher in Cav-$1^{-/-}$ mice, suggesting that resident structural cells may contribute to basal pro-fibrotic inflammation. We observed no difference in serum immunoglobulin levels, indicating Cav-$1^{-/-}$ mice were not "allergic" nor was the innate immune system affected. Our data indicate that Cav-1 may regulate mechanisms, such as Rho/Rho kinase signaling, that determine airway smooth muscle contraction and airway fibrosis; thus, it could be an important regulator of airway biology and physiology in health and disease.

II. Objectives and Rationale

Asthma is one of the most prevalent chronic conditions affecting Canadians today and is a significant cause of morbidity worldwide. According to the 2000 report from the National Asthma Control Task Force, in Canada, it is estimated that 10% of children and 5% of adults have active asthma; however, the prevalence is ever increasing [1]. Unfortunately, this trend is not isolated to Canada. Worldwide rates are, on average, increasing by 50% every decade. The disease imposes a great financial burden on the nation's health care expenditure and accounts for approximately 600 million dollars each year in direct costs alone [1]. It is the major cause of hospitalization and school absenteeism in children and causes a significant limitation of productivity in affected adults. While the disease can cause a reduction in lifespan, its major effect is on the quality of life of affected individuals. Current therapies are directed towards relieving symptoms and have little effect on disease progression. As a result, morbidity increases in individual patients with disease progression. It is therefore becoming increasingly important to understand the cellular mechanisms which contribute to asthma pathogenesis.

Airway responsiveness is controlled primarily by contraction of airway smooth muscle that encircles the bronchi. Airway hyperresponsiveness (AHR) to inhaled spasmogens such as methacholine is a cardinal feature of asthma and is an essential diagnostic index. Current first line reliever medication for asthma, inhaled β2-agonists, are designed to induce airway smooth muscle relaxation and reverse acute bronchoconstriction associated with asthma attacks. Moreover, first line preventer medication for asthma aims to suppress chronic intermittent airway inflammation that underpins development of airway remodeling; a process which includes increased airway fibrosis and airway smooth muscle hypertrophy that result in fixed airway dysfunction. In this regard, there has been considerable research focus in the field on

understanding factors that control airway smooth muscle contractile responses and development of airway remodeling, and how these are associated with asthma pathogenesis.

Caveolae are flask shaped plasma membrane invagination that are highly abundant in many lung cell types, including airway smooth muscle, fibroblasts, endothelial cells and type I pneumocytes. These structures are characterized by an inner membrane protein network composed chiefly of a specialized family of proteins, the caveolins. Three caveolins, caveolin (Cav)-1, -2 and -3, are encoded by different genes, and Cav-1 is the primary family member expressed by human airway smooth muscle cells [2]. Cav-1 includes a unique scaffolding domain that serves as a docking site for a diverse set of intracellular signaling proteins that control key cell processes. Indeed, caveolae are linked with regulation of airway smooth muscle contraction, proliferation and phenotype expression [3-6]. In addition, Cav-1 reportedly regulates age-related changes in lung mechanics as well as lung fibrotic responses and inflammation in response to allergen exposure [7-8]. On this basis, our study focuses on the interactions of Cav-1 that regulate mechanisms contributing to airway smooth muscle contraction, fibrosis, inflammation and overall asthma pathogenesis.

III. Literature Review

Asthma

Asthma is a chronic disease of the airways that causes significant morbidity in both children and adults worldwide. Asthmatics suffer from recurrent episodes of wheezing, chest tightness, breathlessness and cough as a result of changes in their airways [1]. It is estimated that 10% of Canadian children and 5% of adults suffer from active asthma and the worldwide prevalence of this disease has been steadily increasing over the past 15 years [1]. While the mortality rates associated with this disease are typically low, the disease causes significant morbidity to sufferers and this translates into an enormous burden on the nation's healthcare resources. The National Asthma Control Task Force report issued in 2000 reported that 44.2% of patients with active asthma have 3 or more asthma related visits to physicians every year, 18% visit the emergency department at least once per year and 5.3% will require hospitalization for their asthma each year [1]. All of these encounters contribute to the high costs asthma imposes on the health care system - currently estimated at approximately 600 million per year [1].

Characteristic Features of Asthma

Asthma has several characteristic features that collectively define it as a disease. These include variable and reversible air-flow obstruction that cause symptoms and intrinsic changes in airway smooth muscle that result in airway hyperresponsiveness (AHR) [1]. While the pathogenesis of the disease has not been fully elucidated, it is well recognized that acute and chronic inflammation in the conducting airways plays an important role in both the pathogenesis and persistence of asthma [9]. The conducting airways in asthmatics are often referred to as being "twitchy," because the smooth muscle contracts too much and too easily [9]. This contraction and

resulting ‘asthma attack’ can occur spontaneously, or in response to a number of environmental stimuli which are generally harmless to others. The increased sensitivity of the muscle to normally harmless stimuli and the increased contractility of the muscle collectively are known as AHR. During an asthma attack, the contraction of smooth muscle surrounding the airway narrows the lumen of the airway, limiting airflow and making breathing difficult; a process known as bronchoconstriction. The airflow obstruction observed in asthma by definition must be reversible; meaning it is relieved with bronchodilator medications that target airway smooth muscle and cause it to relax. In fact, in order for asthma to be diagnosed, reversible airway obstruction must be demonstrated informally through the relief of symptoms with bronchodilator use or formally with pulmonary function testing. However, to properly diagnose asthma, clinical symptoms must be assessed, airway function should be measured objectively, response to therapy should be monitored and occasionally provocative testing may be required [1].

The contraction of the airway smooth muscle (bronchoconstriction) represents the reversible component of the disease. Current asthma therapies, such as β adrenergic agonists, focus on reversing these asthma attacks by targeting the smooth muscle, causing it to relax. These medications are collectively referred to as ‘relievers.’ Additional therapies, such as corticosteroids, target the underlying airway inflammation as a means of attempting to prevent or reduce the frequency and severity of these episodes. These medications are collectively referred to as ‘preventers.’ While these medications aim to control and suppress asthma symptoms, there are currently no medications that have been shown to be effective at preventing or reversing the disease process. Furthermore, with disease progression, remodeling of the airways can occur that causes irreversible loss of lung function and contributes to the chronic airway hyperresponsiveness in long-time asthma sufferers [10]. Currently there are no therapies proven to prevent or reverse this remodeling process.

Asthma Pathogenesis

Atopic or allergic asthma is the most common form of asthma, especially in children, and in genetically susceptible individuals is thought to develop from repeated exposure to environmental allergens, such as ragweed pollen, house dust mite and animal hair [11]. Exposure to these allergens results in a sensitization of the immune response in some individuals and this sensitization drives the pathogenesis of asthma. For many patients, the disease develops in infancy and is influenced by both genetic (atopy) and environmental factors (exposure to respiratory viruses, airway polluntants and allergens). In these genetically predisposed or atopic individuals, the exposure to environmental factors invokes a type I hypersensitivity reaction that results in the generation of immunoglobulin E (IgE) antibodies against common environmental allergens. Thus, some atopic asthmatics are found to have increased IgE serum levels and may exhibit positive skin-prick tests. However, there are far more atopic individuals than there are atopic asthmatics so the question arises – why do some atopic individuals express their atopy in the conducting airways while other highly atopic individuals have no evidence of asthma?

Allergic Sensitization

One explanation may involve varying immune response to inhaled environmental stimuli. In atopic asthma, the airway recognizes environmental allergens and generates a Th2 cytokine response against them [9, 12]. However, other environmental stimuli, such as rhinovirus infection, environmental tobacco smoke, and other airborne pollutants, have also been shown to be important in initiating the sensitization process that underpins the pathogenesis of asthma [9, 13]. For example, a recent study by Jackson et al. demonstrated that individuals who have repeated infections with rhinovirus during the first 3 years of life have a much greater risk (26 fold) of developing asthma by the age of 6 compared with allergic sensitization (3 fold increased

risk) [13-14]. During sensitization, inhaled allergens encounter dendritic cells in the airway epithelium. The dendritic cells then migrate to the lymph nodes to present the antigen (allergen, virus, etc) to T and B lymphocytes [12]. The nature of the immune response is dependent upon which co-stimulatory molecules are activated [9]. Through complex interactions involving cytokines (interleukins (IL-) 4 and 13) and cell surface markers (CD40 and B7) on B and T cells, IgE is synthesized and released from B cells [12]. Sensitized T cells then migrate back to the airways and become potent producers of a variety of pro-inflammatory cytokines. The circulating IgE will bind to high affinity receptors on mast cells and low affinity receptors on lymphocytes, eosinophils and macrophages [12]. Once sensitized, re-exposure to the same allergen can invoke an asthma attack through crosslinking to IgE antibodies bound to the surface of sensitized mast cells interspersed among airway epithelium [12]. This interaction causes mast cells to degranulate and release a variety of inflammatory mediators (histamine, tryptase, cytokines, and eicosanoids including thromboxane A_2 and leukotrienes), that lead to airway smooth muscle contraction, mucus hypersecretion and edema, all of which contribute to the airway obstruction [9, 12]. This initial attack is referred to as the early phase reaction and will usually resolve within an hour or with recovery medication. The release of inflammatory mediators during the early phase reaction also recruits eosinophils and neutrophils to the lung [11]. A late phase reaction is often also experienced, 4-6 hours later, as a result of the cytokines released from resident structural cells (macrophages, mast cells and epithelial cells) as well as the recruited inflammatory cells (lymphocytes and eosinophils) [12]. Eosinophils are particularly important in asthma because their activation leads to the release of more inflammatory mediators which cause tissue damage, can further bronchoconstriction and contribute to the chronic inflammation in long time asthma sufferers [9, 15]. In fact, other inflammatory airway diseases such as bronchitis are distinct from asthma because the cytocellular inflammation in these diseases is not primarily eosinophilic in

nature [11, 15]. Thus, it is recognized that the underlying inflammation seen in atopic asthma underpins a significant portion of the associated symptoms of the disease and varying sensitization immune responses may partly explain why some atopic individuals do not exhibit asthma symptoms.

The Epithelial- Mesenchymal Trophic Unit and Airway Remodeling

An additional theory behind the pathogenesis of atopic asthma revolves around differences in structure and function of epithelium in the airways. Bronchial biopsies taken from asthmatic airways show dramatic changes to the airway epithelium compared with normal bronchial samples. Some of these changes are present at the beginning of the disease, perhaps even before diagnosis in childhood, possibly indicating an intrinsic difference in the airways of asthmatics [9, 16-17]. Even in the mildest forms of asthma, there is evidence of structural change including epithelial metaplasia and damage, thickening of the basement membrane (lamina reticularis), and increased number of myofibroblasts [9, 16, 18-20]. Additional changes to the airway wall, such as airway smooth muscle thickening and angiogenesis, originally thought to be in response to chronic inflammation, are being described in children at the time of diagnosis [16]. These changes have collectively been termed airway remodeling and will be discussed further below. The changes seen suggest that the airway epithelium in asthmatics exists in a chronically injured state and recent studies showing impaired proliferation indicate that the damaged epithelium is unable to properly repair itself [9, 21-22]. Histological examination reveals epithelial damage with loss of columnar cells and disruption of tight junctions and desmosomal attachments [9, 16]. These changes significantly increase the permeability of the asthmatic epithelium which may allow inhaled allergens, respiratory viruses and pollutants greater access to the deeper structural cells and immune cells, triggering enhanced signaling between these cells that causes abnormally

destructive responses [9, 13]. This interaction, between the epithelium and the underlying mesenchyme, has been named the epithelial-mesenchymal trophic unit and is believed by some to drive the pathogenesis of asthma. To further explain, the defect in epithelial barrier function could potentially promote allergic sensitization and explain why some atopic individuals become sensitized and others do not. Furthermore, it has been suggested that activation of the epithelial-mesenchymal trophic unit in conjunction with the epithelium's inability to properly repair itself, may result in aberrant repair mechanisms that lead to a remodeling of the airway and further disease progression [9, 13].

Airway remodeling refers to the irreversible changes that occur to the formed elements of the airway with chronic airway inflammation and disease progression. It involves changes in the composition, quantity, content and organization of the cellular and molecular constituents of the airway wall [19-20]. More specifically, the structural changes include airway smooth muscle hyperplasia and hypertrophy, mucus gland and goblet cell hyperplasia, angiogenesis, subepithelial fibrosis and altered deposition and composition of extracellular matrix (ECM) and proteoglycans [9-10, 19-20]. While the structural changes that occur to the airways in asthmatics have been well documented and recognized, the cellular and molecular mechanisms that drive these changes are still being researched. The end result of airway remodeling is an overall thickening and 'stiffening' of the airway wall that produces persistent, irreversible airflow obstruction, and accelerated decline in lung function over time [10, 13, 23]. Thus, as the disease progresses and the airway remodels, bronchoconstriction and airflow limitation becomes increasingly difficult to reverse with conventional pharmacological therapies and treatment may become refractory. As there are no current therapies to prevent or reverse this remodeling process, it is becoming increasingly important to better understand the cellular mechanisms that drive airway remodeling, so that new therapies can be developed. Our study demonstrates that the

protein Cav-1 plays a key role in regulating mechanisms such as airway smooth muscle contraction, fibrosis and inflammation that may contribute to airway remodeling and overall asthma pathogenesis.

Caveolae and the Caveolin Gene Family

Caveolae were discovered by Palade in 1953, but did not receive their name until 1955 [24]. They were first described as "plasmalemmal vesicles" and were later termed caveolae because of their resemblance to "little caves" in the membrane [24-25]. These structures are formed through the invagination of the plasma membrane and have a characteristic Ω-shape (Figure 1). They measure 50-100nm in diameter and represent a subclass of lipid rafts enriched in cholesterol and sphingolipids [26]. Caveolae are abundant in many cells including fibroblasts, adipocytes, endothelial and epithelial cells, as well as smooth and striated muscle, suggesting they play an important role in cell physiology [27-29]. Indeed, caveolae have a role in diverse cellular functions including endocytosis, membrane trafficking, cell signaling and cholesterol homeostasis [26, 30-31]. Their presence is dependent upon the expression of specific scaffolding proteins, the caveolins, which bind to cholesterol and sphingolipid enriched microdomains in the membrane and anchor them to the cytoskeleton [32].

To date, three caveolins have been identified: caveolin-1, caveolin-2 and caveolin-3. The caveolin gene family is conserved both structurally and functionally from *Caenorhabditis elegans* to humans, supporting the idea that these proteins are essential for normal cellular function [33-35]. Caveolin-1 (Cav-1) and cav-2 are co-expressed in many tissues, but the highest

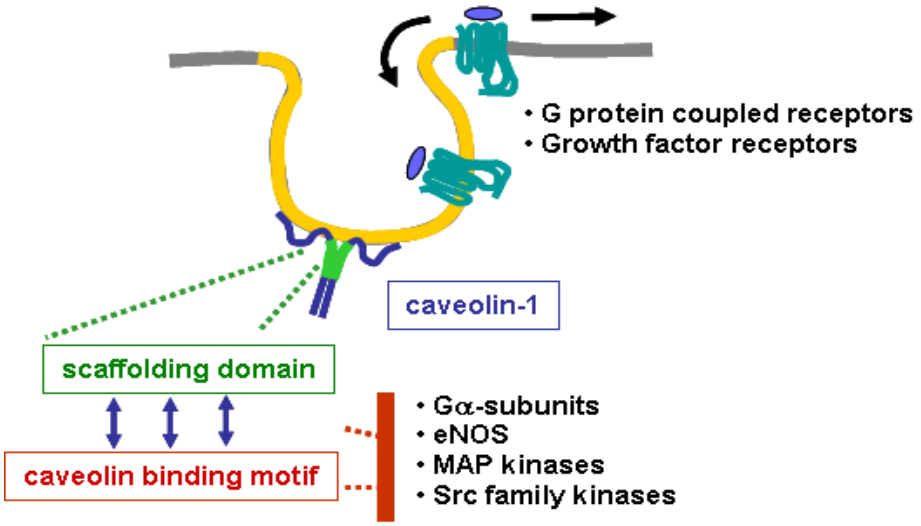

Figure 1: Structure and functional domains of caveolae. Caveolae are plasma membrane (grey) invaginations which are associated with G protein coupled receptors and growth factor receptors (teal). These receptors are able to move in and out of the caveolae allowing for activation of other signaling molecules co-localized in caveolae (not shown). Caveolin-1 (dark blue) is a scaffolding protein which causes the formation of caveolae through its association with cholesterol (yellow). The scaffolding domain of caveolin-1 (green) binds to the caveolin binding motif (red) of several intracellular signaling molecules (Gα subunits, eNOS, MAP kinases, Src kinases) resulting in the inhibition of downstream signaling.

levels are found in endothelial cells, epithelial cells, adipocytes, fibroblasts and smooth muscle cells [27, 29]. In contrast, cav-3 expression is generally expressed primarily in skeletal and cardiac muscle cells, although some studies report its expression in smooth muscle as well [27, 36-37]. Of the three caveolin proteins, Cav-1 is the most extensively characterized. It is a 22-24 kDa intracellular cell membrane associated protein which binds cholesterol with high affinity and can induce caveolae formation when over expressed in cell lines. In fact, it is the sole caveolin protein required for caveolae formation [32, 38]. Cav-1 has been implicated as a regulator of signal transduction pathways due to the presence of a large (20 amino acids) caveolin scaffolding domain (Figure 1) [39]. This domain is capable of binding to various intracellular signaling molecules including H-Ras, Src family tyrosine kinases (c-Src), receptor tyrosine kinases, endothelial nitric oxide synthase (eNOS) and the α-subunit of heterotrimeric G-proteins to

regulate their activity [30]. In general, the interaction of the cav-1 scaffolding domain with caveolin-binding domains in these proteins results in the inhibition of downstream signaling [28]. Following an appropriate stimulus, Cav-1 and the signaling molecule disassociate, allowing for the propagation of downstream signaling. For example, it is well known that caveolae regulate eNOS activity in the cardiovascular system. eNOS is inactivated when bound to cav-1; however, when intracellular calcium levels increase, eNOS is displaced from Cav-1 resulting in the production of nitric oxide (NO), resulting in vasodilation [40-42]. The interaction of Cav-1 with these various signaling molecules can have important biological consequences in the lung as recent evidence links Cav-1 to signaling pathways that drive lung inflammation [43], lung fibrosis [44], and contraction of isolated airway smooth muscle preparations [6, 45].

Caveolin-1 Knockout Mice

The recent availability of genetically engineered, caveolin-1 knockout (Cav-$1^{-/-}$) mice has provided the opportunity to study the *in vivo* role of this protein using whole animal models. The CAV1 gene is silenced in these animals by targeted disruption of exons 1 and 2, and results in the loss of caveolae [31]. When Cav-1 is absent, the arrangement of cholesterol in lipid rafts is destabilized and caveolae structures cannot form [46-47]. Despite the widespread expression of Cav-1, mice deficient in the protein are both viable and fertile. Nonetheless, Cav-$1^{-/-}$ mice exhibit a ~50% reduction in life span [48] marked by a major decline in viability occurring between 27-65 weeks that is attributable to pulmonary fibrosis, pulmonary hypertension and cardiac hypertrophy [48]. As expected, Cav-$1^{-/-}$ mice demonstrate morphological defects in several organ systems. The lungs exhibit a marked reduction in alveolar area and thickened alveolar septae arising from the development of multilayered alveolar walls [30-32, 38, 48]. Cav-$1^{-/-}$ mice display a reduced ability to perform physical work, demonstrated by early fatigue during forced

swimming stress, a phenotype that is likely attributable to vascular dysfunction and lung defects [32]. Interestingly, the alveolar spaces of Cav-$1^{-/-}$ mice contain numerous extravasated red blood cells suggesting an endothelial defect that leads to vascular leakage [32]. Enhanced staining for cell proliferation (Ki67) and non-differentiated endothelial cell (Flk-1) markers reveal marked peripheral lung hypercellularity due to endothelial cell hyperplasia [32, 48]. In addition, azan staining and electron microscopy analyses reveal a significant increase in extracellular fibrillar deposits in the alveolar interstitium of Cav-$1^{-/-}$ mice [32]. These data indicate Cav-1 is likely an important regulator of proliferative and fibrotic responses throughout the lung. The abundance of caveolae in the lung, the associations with smooth muscle function and cell proliferation, and the histological abnormalities associated with the loss of Cav-1, suggests a more rigorous assessment of lung physiology is required. This is a key focus of the current research project.

Caveolae in Human Disease

Caveolin-1 mutations have been associated with numerous human diseases such as cancer, diabetes, and atherosclerosis [30]. While the majority of research involving Cav-1 has focused on associations with vascular diseases and cancer, evidence suggests this protein is also likely involved in respiratory diseases, such as asthma. Cav-1 is expressed abundantly by lung cells, such as airway smooth muscle, the epithelium, and type I pneumocytes [27]. It is also well established that epithelial cells and airway smooth muscle contribute to local inflammation via caveolae associated receptors for external signals such as growth factors and viral infection [49]. Secondly, Cav-1 regulates receptor mediated airway smooth muscle cell responses through their association with G protein coupled receptors [49-50]. These responses include contraction and proliferation, processes that contribute to the development of airway hyperresponsiveness and airway remodeling. A functional role for caveolae and Cav-1 in the key cells that control airway

responses and inflammation, suggests the protein could modulate important aspects of asthma pathogenesis and morbidity.

Caveolin-1 and Fibrosis

Fibrosis is defined as the formation of excess fibrous connective tissue in an organ or tissue as part of a reparative or reactive process. In the lung, pulmonary fibrosis can occur as a secondary process associated with other lung diseases (asbestosis, autoimmune diseases, infections) or as an independent idiopathic process (idiopathic pulmonary fibrosis). At a cellular level, it is believed that lung fibrosis is driven by interactions between epithelial cells and fibroblasts. Activated epithelial cells recruit immune cells and together they release a variety of pro-fibrogenic molecules and cytokines such as tumor necrosis factor α (TNF-α) and transforming growth factor β 1 (TGF-β1) that promote the activation of fibroblasts into a myofibroblast state [51]. TGF-β1 further stimulates these myofibroblasts to increase production of extracellular matrix (ECM) proteins, such as collagen type I and fibronectin, which contribute to the matrix deposition in the lung parenchyma. A cycle of lung injury and repair perpetuates and eventually leads to progressive fibrosis and loss of lung parenchyma that significantly impairs lung function.

Interestingly, it has been shown that similar signaling mechanisms contribute to the subepithelial airway fibrosis and basement membrane thickening that occurs with airway remodeling in asthma. Recent studies suggest Cav-1 may actually play a protective role in this fibroproliferative process through its regulation of TGF-β1 signaling [52-56]. For example, lung tissue from patients with idiopathic pulmonary fibrosis demonstrated reduced levels of Cav-1 expression, particularly in alveolar epithelial cells and lung fibroblasts, suggesting that Cav-1 may have a protective role in preventing fibrotic changes to the lung [44]. In further support of

this role, when Cav-1 was administered intra-tracheally, it conferred resistance to a bleomycin-induced lung fibrosis in mice [44, 57]. At a molecular level, it has been shown that Cav-1 suppresses TGF-β signaling by altering TGF- β receptor expression and preventing receptor mediated induction of Smad signaling cascades that can drive collagen expression [58-59]. In addition to suppressing the production of ECM proteins that contribute to fibrosis, Cav-1 also regulates the proliferation of fibroblasts and airway smooth muscle cells. Spontaneous mitosis can be induced by Cav-1 gene silencing [5, 60] whereas overexpression of Cav-1 induces cell cycle arrest in fibroblasts and can prevent growth factor induced smooth muscle proliferation [33, 61]. Thus Cav-1 appears to be heavily involved in the regulation of signaling pathways that contribute to ECM protein production and fibrotic processes.

Recent studies by Le Saux et al further support the role of Cav-1 in regulating fibroproliferative processes involved in airway remodeling [7-8]. Their studies demonstrated that allergic sensitization and challenge significantly reduces Cav-1 expression and caveolae formation in murine lung tissue. This reduction in Cav-1 was associated with enhanced TGF-β signaling, and increased collagen deposition surrounding the airways as well as in the lung parenchyma, detected by trichrome staining [7]. An additional study by the same group demonstrated that this altered signaling likely contributes to changes in the mechanical properties of the lung. This study demonstrated that Cav-$1^{-/-}$ mice have reduced lung compliance (and thus increased elastance; the inverse of compliance) and increased airway resistance by 3 months of age [8]. The changes in compliance and elastance were attributed to enhanced deposition of collagen fibrils and elastin fibres in the airways and parenchyma of the lungs [8]. Thus, Cav-1 appears to be a key regulatory protein in controlling fibrotic changes in the airways and parenchyma of the lung and therefore likely contributes to the remodeling process.

Smooth Muscle Contraction

Muscle contraction is made possible through the interaction between myosin and actin filaments in the muscle cell. These molecules interact to form cross bridges that drive contraction in cardiac, skeletal and smooth muscle cells. Myosin heads will bind to neighbouring actin filaments to form these cross-bridges and once bound, the myosin head will undergo a conformational change and pivot to generate a power stroke that pulls the actin filament towards the center of the myosin molecule [62-64]. Since actin filaments are anchored to additional structural elements of the cell, the movement of the actin filament results in a change in cell length and force is generated [65-66].

While the interaction between actin and myosin is similar amongst all muscle cells, the regulation of this interaction differs greatly between smooth and striated muscle. In striated muscle, most of the regulation of contraction is the responsibility of the thin actin filament, whereas contraction in smooth muscle is regulated by signaling pathways that target the thick myosin filament [66]. Thus, smooth muscle contraction is the end product of multiple intracellular signaling that act on the myosin light chain (MLC_{20}) and lead to its phosphorylation which facilitates its interaction with actin to form cross bridges and generate force (Figure 2). The subsequent force generated through myosin-actin cross bridge cycling directly correlates with the level of phosphorylated MLC_{20} and two proteins operate antagonistically to regulate the phosphorylation process [67]. Myosin light chain kinase (MLCK) acts to phosphorylate MLC_{20} while myosin light chain phosphatase (MLCP) will dephosphorylate MLC_{20}. The overall level of contraction thus depends on the level of activity of the intracellular signaling mechanisms that modulate MLCK or MLCP activity [68].

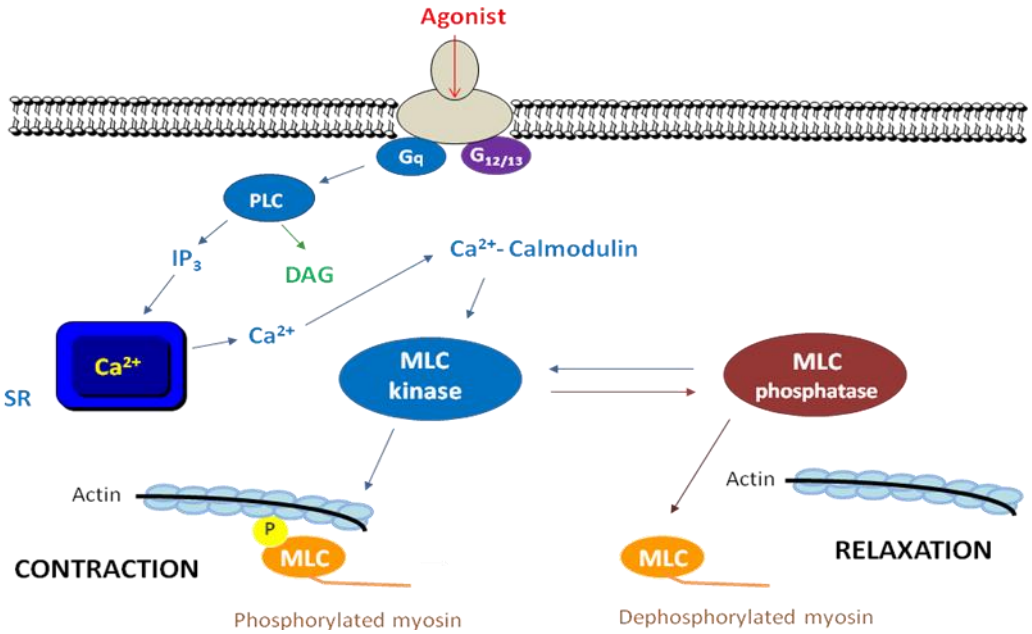

Figure 2: Calcium (Ca^{2+}) dependent mechanisms of smooth muscle contraction. When an agonist binds to a G protein coupled receptor (grey), downstream signaling leads to the activation of phospholipase C (PLC) that cleaves phosphotidylinositol biphosphate into inositol triphosphate (IP_3) and diacylglycerol (DAG). IP_3 binds to receptors on the sarcoplasmic reticulum (SR) resulting in Ca^{2+} release [69]. The strength of contraction is dependent on the intracellular Ca^{2+} level and is therefore said to be Ca^{2+} dependent. Intracellular Ca^{2+} binds to calmodulin and the Ca^{2+}-calmodulin complex activates myosin light chain (MLC) kinase which in turn phosphorylates (P) the myosin light chain (MLC) [69]. Phosphorylated MLC is able to interact with actin to form crossbridges, resulting in smooth muscle contraction. The strength of contraction also depends on the level of activity of MLC phosphatase, an enzyme which de-phosphorylates MLC. Dephosphorylated MLC is unable to interact with actin; thus, MLC phosphatase promotes smooth muscle relaxation.

The predominant pathway for initiating contractile responses involves an increase in intracellular calcium (Ca^{2+}) and as such, these pathways are referred to as Ca^{2+} dependent contractile pathways (Figure 2). At rest, Ca^{2+} concentrations in the extracellular space and within the sarcoplasmic reticulum are approximately 10,000 times greater compared to the intracellular levels of unbound/free Ca^{2+} [70]. Cytoplasmic levels of free Ca^{2+} are so tightly controlled because Ca^{2+} regulates multiple intracellular signaling pathways that result in programmed cell death (apoptosis), proliferation, transcriptional activation, adherence, migration, and secretion. Because of its involvement in these different pathways, there are many stimuli that are able to augment intracellular Ca^{2+} concentrations. Mechanisms that can raise Ca^{2+} levels in smooth

muscle include stretching the cell, electrical stimulation leading to membrane depolarization and Ca^{2+} influx, and nervous or hormonal production of molecules that open ion channels on the cell membrane or interact with G-protein coupled receptors [70]. The increase in intracellular calcium will lead to binding to calmodulin and the Ca^{2+}-calmodulin complex activates MLCK, resulting in myosin light chain phosphorylation, cross-bridge formation and subsequent contraction.

Additional pathways control contraction through the modulation of MLCP activity and collectively, these pathways are often termed Ca^{2+} independent contractile pathways. They can increase smooth muscle contraction at a fixed intracellular Ca^{2+} level, through the inhibition of MLCP. To date, there are three known mechanisms of MLCP inhibition targeted by these pathways: phosphorylation of the 110-130 kDa regulatory subunit called the myosin phosphatase-targeting subunit (MYPT1), arachidonic acid-induced dissociation of the holoenzyme, and the inhibition of the 37 kDa catalytic subunit (PP1c) by phosphorylated CPI-17 [67, 69]. Protein kinase C (PKC), RhoA/Rho kinase (ROCK1/2) and ERK1/2 signaling represent three Ca^{2+} independent pathways which promote smooth muscle contraction (Figure 3) [67, 71]. The activation of RhoA/ROCK1/2 and/or ERK1/2 signaling results in the phosphorylation of MYPT1; whereas, the activation of PKC signaling results in the phosphorylation of CPI-17 and subsequent inhibition of PP1c. In addition, through a PKC dependent mechanism, ERK1/2 can phosphorylate caldesmon, a protein which normally binds actin to prevent its interaction with myosin. When phosphorylated, the inhibitory action of caldesmon is reversed and contraction is achieved.

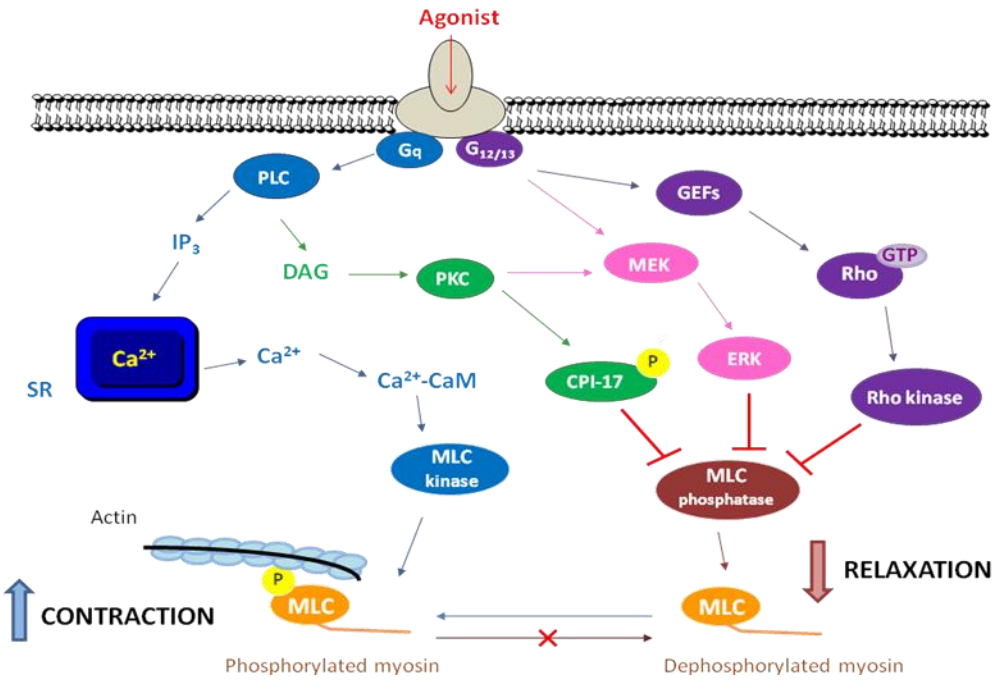

Figure 3: Calcium (Ca^{2+}) independent mechanisms of smooth muscle contraction. In addition to Ca^{2+} dependent mechanisms (blue), there are several mechanisms that can enhance smooth muscle contraction independent of intracellular Ca^{2+} levels. Activated phospholipase C (PLC) converts phosphotidylinositol biphosphate into inositol triphosphate (IP_3) and diacylglycerol (DAG) [69]. IP_3 is involved in Ca^{2+} dependent smooth muscle contraction, but DAG can activate protein kinase C which has many downstream effects (green). Activated PKC phophorylates CPI-17 leading to the inhibition of the catalytic subunit on myosin light chain (MLC) phosphatase [69]. In addition, PKC can activate the MEK/ERK 1/2 mitogen activated protein pathway (pink) which phosphorylates and inhibits the regulatory subunit of MLC phosphatase. The Rho/Rho kinase pathway (purple) is the final Ca^{2+} independent mechanism of smooth muscle contraction depicted above. When an agonist binds to a G protein coupled receptor (grey) a G protein (G_{12}/G_{13}) is activated. Guanine nucleotide exchange factors (GEFs) provide a direct link between the G protein and the small GTPase Rho [69]. Similar to PKC, activated Rho kinase will phosphor ylate and inhibit the regulatory subunit of MLC phosphatase. The inhibition of MLC phosphatase prevents the dephosphorylation of MLC. This indirectly leads to an increase in MLC kinase activity and an increase in the levels of phosphorylated MLC; thus, smooth muscle contraction increases.

Caveolae and Smooth Muscle Contraction

Caveolae appear to be involved in both Ca^{2+} dependent as well as Ca^{2+} independent pathways of smooth muscle contraction. Numerous studies have demonstrated that caveolae likely play a role in the regulation of intracellular Ca^{2+} concentration ($[Ca^{2+}]_i$) that leads to smooth muscle contraction. In airway smooth muscle, hormones and neurotransmitters, such acetylcholine (ACh), histamine and bradykinin, stimulate contraction and bronchoconstriction leading to

increased airway resistance through pathways that raise $[Ca^{2+}]_i$ (Ca^{2+} dependent pathways). When these bronchoconstricting agents bind to their receptors in the plasma membrane, they trigger Ca^{2+} release from SR stores and Ca^{2+} influx across the plasma membrane through voltage gated and receptor gated channels [45, 72-73]. Cav-1 and caveolae appear to be directly involved in regulating these responses to bronchoconstricting agonists through interactions with the receptors for these agents. For example, there is increasing evidence that caveolae contain key components for Ca^{2+} handling (L-type Ca^{2+} channels, Ca^{2+} binding proteins and the plasma membrane Ca^{2+} pump) and may actually serve as initiation sites for Ca^{2+} sparks that trigger smooth muscle contraction [2, 74]. Furthermore, it has been demonstrated in vascular smooth muscle, that caveolae are located in close proximity to the SR, a key intracellular organelle involved in regulating $[Ca^{2+}]_i$ [2, 75]. Previous studies from our lab demonstrated that the receptors for some of these bronchoconstricting agents, in particular ACh muscarinic receptors, are located within caveolae and will co-fractionate within Cav-1 rich membranes in ASM [6]. We further demonstrated that when caveolae are disrupted by cholesterol depletion with methyl-β cyclodextrin, Cav-1 binding capacity is disrupted with cell permeable Cav-1 scaffolding domain or Cav-1 expression is diminished with the small interfering RNA, the $[Ca^{2+}]_i$ responses and the force induced by ACh stimulation are severely disrupted. In particular it was noted that in the absence of functional Cav-1, the maximum isometric force generated and the maximum $[Ca^{2+}]_i$ responses induced by ACh were not altered; however, the sensitivity to ACh was diminished [6]. Interestingly, fluorescence microscopy demonstrated that in canine and human ASM cells treated with methyl- β cyclodextrin, Cav-1 and the ACh receptor M3R no longer co-localized in the absence of functional caveolae; however, the loss of Cav-1 had no apparent effect on the availability or affinity of these receptors [6]. Thus it would appear that Cav-1

interacts with ACh receptors to regulate downstream signaling leading to $[Ca^{2+}]_i$ responses that drive smooth muscle contraction. An additional study by Prakash et al further supported our previous findings. Their study involved responses to several bronchoconstricting agonists (ACh, histamine, bradykinin) and they again demonstrated that the receptors for these agents co-localize with Cav-1 and caveolae in the plasma membrane of human ASM cells. They also demonstrated altered $[Ca^{2+}]_i$ responses with disruption of Cav-1 and caveolae in response to ACh, histamine and bradykinin stimulation [45]. These studies suggest that in the absence of caveolae, the receptors, second messaging systems and ion channels may remain semi-functional; however, caveolae and Cav-1 seem to coordinate these functions during excitation-contraction coupling to lead to an increase in to $[Ca^{2+}]_i$ that facilitates contraction.

With regards to regulating Ca^{2+} independent smooth muscle contraction, the interaction between caveolae and both PKC and RhoA/ROCK1/2 signaling is well documented. It has been demonstrated *in vitro* that PKC-α and RhoA translocate to the membrane and associate with caveolae upon membrane receptor stimulation [76-77]. More specifically, it has been shown that upon this translocation, both PKC-α and RhoA directly interact with Cav-1. Interestingly, it has been demonstrated in intestinal, vascular and colonic smooth muscle that the loss of Cav-1 alters contraction via PKC and/or Rho kinase signaling [37, 67, 78]. Shakirova et al demonstrated that longitudinal muscle from the ileum of Cav-$1^{-/-}$ mice shows enhanced contractility and enhanced RhoA signaling [37]. A similar mechanism may occur in airway smooth muscle however no studies have been completed using ASM thus far. To date, it is unclear if Cav-1 regulates ERK1/2 dependent contractile pathways; however, previous studies have described an association between these proteins with additional downstream effects. Taken collectively, these

results suggest that caveolae and Cav-1 appear to play an essential role in smooth muscle contraction through their association with Ca^{2+} dependent and independent contractile pathways.

Caveolin-1 and Inflammation

Cav-1 has also been shown to have anti-inflammatory effects [43, 79-80]. For example, in murine alveolar macrophages, Cav-1 regulates LPS-induced cytokine production through its suppressive effects on the MKK3/p38 mitogen-activated protein kinase (MAPK) pathway, and on nuclear factor-κB (NF-κB) and activator protein-1 (AP-1) activation [43]. Moreover, silencing of Cav-1 expression by small interfering RNA (siRNA) results in increased production of Th2-polarized pro-inflammatory cytokines (TNF-α and IL-6) and decreased production of IL-10, a Th1 cytokine, in response to LPS stimulation [43]. Importantly, over expression of Cav-1 abrogates the effects of Cav-1 siRNA on TNF-α, IL-6 and IL-10 in response to LPS [43]. Collectively, these data suggest Cav-1 acts as a suppressor of inflammation, and regulates the fibrotic and proliferative activities of multiple lung cell types *in vitro* and *in vivo*.

IV. Hypotheses and Specific Aims

To date, the focus has been on Cav-1 interactions in the peripheral lung. As a result, there is a paucity of quantitative and functional data related to the airways of Cav-$1^{-/-}$ mice. Of note, the airways, similar to the peripheral lung, demonstrate hallmark fibroproliferative changes in association with chronic inflammatory lung diseases such as asthma and chronic obstructive pulmonary disease (COPD) and Cav-1 likely has a role in these processes as well. There is an obvious link between Cav-1 and both lung fibrosis and inflammation that is evident in Cav-$1^{-/-}$ mice, but there is limited evidence reported to date that systematically characterizes respiratory mechanics and airway function in response to methacholine challenge in these mice. Furthermore, there is a lack of evidence characterizing the contractile properties of the airway smooth muscle *in vivo* and *ex vivo* in these animals. We performed several experiments to answer the following hypotheses:

1. We measured respiratory mechanics in Cav-$1^{-/-}$ and B6129SF2/J mice following a methacholine challenge. **We hypothesized that Cav-$1^{-/-}$ would demonstrate enhanced airway reactivity and tissue elastance compared to the controls based on previous study findings** [8].

2. We used morphometric analyses to characterize changes in both smooth muscle mass as well as collagen deposition in central and peripheral airways of Cav-$1^{-/-}$ mice. **We hypothesized that Cav-$1^{-/-}$ mice would exhibit increased collagen deposition and smooth muscle mass surrounding central and peripheral airways compared with their wild type controls (B6129SF2/J)**.

3. To correlate fibroproliferative changes with underlying inflammation in naïve mice, we collected brochoalveolar lavage fluid (BALF) to analyze inflammatory cell number and differentials as well as perform ELISA for pro-inflammatory cytokines. We also assessed immune status by measuring serum immunoglobin levels. **We hypothesized that Cav-1$^{-/-}$ mice would show no differences in inflammatory cell profile or serum immunoglobin levels, but that they would demonstrate elevated levels of pro-inflammatory cytokines that regulate collagen deposition and airway smooth muscle proliferation.**

4. We assessed airway smooth muscle contraction by myography to identify any differences in airway smooth muscle sensitivity or reactivity to methacholine between mouse strains. **Based on our findings *in vivo*, we hypothesized that Cav-1$^{-/-}$ mice would demonstrate enhanced ASM reactivity to methacholine compared to their wild type controls (B6129SF2/J).**

5. Based on the findings of the experiments listed above, we aimed to determine the signaling pathways responsible for the lung mechanics and myography results demonstrated. Multiple studies have suggested interactions between Cav-1 and PKC, ERK1/2 and Rho kinase can regulate smooth muscle contraction. We investigated the involvement of each of these pathways in the airway smooth muscle properties elicited in Cav-1$^{-/-}$ mice *ex vivo*. **We hypothesized that enhanced Rho kinase signaling was the likely cause of altered airway smooth muscle contraction in Cav-1$^{-/-}$ mice.**

V. Materials and Methods

Animals

Female Cav-1$^{-/-}$ mice (7-8 weeks old) were purchased from Jackson Laboratory (Bar Harbor, Maine, USA). To confirm the genotype of each knock out mouse, PCR analyses of DNA extracted from tails was performed using primers and conditions described by Jackson Laboratories. As recommended by Jackson Laboratories, female, 7-8 week old B6129SF2/J mice were used as genetic control for all studies. Female C57BL/6 mice (7-8 weeks old) were purchased from the University of Manitoba Central Animal Care Services (Winnipeg, MB). Mice were maintained on regular laboratory chow, and 12 hour dark and light cycle. One week acclimatization period was given after arrival before any procedures were done. All procedures in this study were performed according to standard operating procedures as per guidelines approved by the animal ethics committee, University of Manitoba.

Preparation of protein lysates from tissues isolated from Cav-1$^{-/-}$ and B6129SF2/J mice for measurement of Cav-1, Cav-2 and Cav-3 protein expression

The diaphragm, heart, small intestine, gastrocnemius muscle, lungs and trachea were isolated from Cav-1$^{-/-}$ and B6129SF2/J mice and homogenized in ice cold RIPA buffer (composition: 40 mM Tris, 150mM NaCl, 1% IgepalCA-630, 1% deoxycholic acid, 1 mM NaF, 5mM glycerophosphate, 1mM Na3VO4, 10 μg/ml aprotinin, 10 μg/ml leupeptin, 7 μg/ml pepstatin A, 1 mM PMSF, pH8.0) using a polytron. Following homogenization, lysates were sonicated 3 times for 10 seconds. The lysate was then centrifuged (760 × g, 5min) and the supernatant stored at -20°C for subsequent protein assay and immunoblot analyses.

Preparation of protein lysates from tissues isolated from Cav-1$^{-/-}$ and B6129SF2/J mice for measurement of RhoA, ROCK1 and ROCK2 protein expression

The lungs and trachea were isolated from Cav-1$^{-/-}$ and B6129SF2/J mice and homogenized in ice cold RIPA buffer (composition: 40 mM Tris, 150mM NaCl, 1% IgepalCA-630, 1% deoxycholic acid, 1 mM NaF, 5mM _-glycerophosphate, 1mM Na3VO4, 10 μg/ml aprotinin, 10 μg/ml leupeptin, 7 μg/ml pepstatin A, 1 mM PMSF, pH 8.0). Lungs were homogenized using a polytron, whereas tracheas were frozen and pulverized. Following homogenization, lysates were sonicated 3 times for 10 seconds. The lysates were then centrifuged (10000g, 10 min) and the supernatants stored at -20°C for subsequent protein assay and immunoblot analyses.

Immunoblotting

Protein content in tissue samples was determined using the BioRad protein assay (BioRad, Hercules, CA) with bovine serum albumin as a reference. Immunoblotting was performed using standards techniques. Briefly, after reconstituting samples in denaturing buffer, 10-15ug protein was loaded per lane and size-separated electrophoretically under reducing conditions using SDS-polyacrylamide gels. Thereafter proteins were electro-blotted onto nitrocellulose membranes, which were subsequently blocked with 5% w/v skim milk in Tris Buffered Saline (TBS) (composition: 10 mM Tris HCl, pH8.0, 150 mM NaCl) with (0.2%) or without Tween-20. Blocked membranes were incubated with primary antibodies (Cav-1 [1:2000], caveolin-2 [1:1000] or caveolin-3 [1:750]; or RhoA [1:250], ROCK-1 [1:250], ROCK-2 [1:250]) diluted in TBS containing 1% w/v skim milk with (0.2%) or without Tween-20. Blots were then incubated with diluted horseradish peroxidase conjugated secondary antibodies prior to visualizing bands on film using enhanced chemiluminescence reagents (Amersham, Buckinghamshire, UK). All

blots were subjected to densitometry using a computer page scanner and TotalLab^{TM} software. For data analyses bands were normalized to β-actin [1:20000] to correct for small differences in loading.

RNA isolation and RT-PCR

Total RNA was extracted using the Qiagen RNeasy Mini Kit in accordance with the manufacturer's recommendations (Qiagen, Mississauga, ON) from tissues isolated from Cav-1$^{-/-}$ and B6129SF2/J mice. Total RNA (1 μg) was reverse transcribed using M-MLV reverse transcriptase (Promega, Madison, WI) for 1 h at 37°C. The RT-PCR reactions for cDNAs of interest were carried out in a thermal cycler (Mastercycler, Eppendorf, Germany) using primer pairs for: Cav-1: forward primer, 5`- CTCCGAGGGACATCTCTACAC – 3`; reverse primer, 5`-GTGCTGATGCGGATGTTGCTG -3`, caveolin-2: forward primer, 5'-CGATGTGCAGCTCTTCATGGC -3`, reverse primer, CGATGCTGACCGATGAGAAGC -3`, and caveolin-3: forward primer, 5`- GATCTGGAAGCTCGGATCATC -3`, reverse primer, 5`-GTGCGGATACACAGTGAGTAG-3`. The coding regions corresponding to the primers were taken from National Center for Biotechnology Information (NCBI) and primers were designed using PRIMER-3 and IDT programs available online. Cycle parameters were: denaturation (94°C for 45 s), annealing (60°C for 45 s), and extension (72°C for 45 s). The initial denaturation period was 4 min and the final extension was 5 min. Glyceraldhyde-3-phosphate dehydrogenase (GAPDH) was amplified as an internal control (GAPDH: forward primer, 5`-AGCAATGCCTCCTGCACCACCAAC -3`, reverse primer, 5`-CCGGAGGGGCCATCCACAGTCT -3`). Amplified products were analyzed by DNA gel electrophoresis in 1.5% agarose, and visualized by Gelstar staining under ultraviolet illumination

using a gel documentation system (AlphaEaseFC, Alpha Innotech Corporation, San Leandro, CA).

Electron Microscopy

Mouse lungs were fixed by gravity-fed intra-tracheal instillation at 23 cmH_2O with 3% glutaraldehyde in 0.1 M phosphate buffer (pH 7.3) for two hours at room temperature. Whole lungs were then cut into small blocks and fixed for an additional one hour at room temperature. Tissues were rinsed overnight at 4°C with 5% sucrose in 0.1M phosphate buffer (pH 7.3). Tissues were then post-fixed in 1% osmium tetroxide in 0.1 M phosphate buffer (pH 7.3) for two hours at room temperature. After dehydration in ascending concentrations of alcohol, tissues were embedded in Epon 812. Thick sections (1μm) were stained with toluidine blue and examined for routine orientation. Thin sections were then prepared and stained with uranyl acetate and lead citrate, before viewing and photography using a Philips CM 10 electron microscope.

Lung Mechanics: Methacholine Concentration-Response Characteristics

For baseline lung mechanics, mice were anesthetized with intra-peritoneal sodium pentobarbital (60 mg/kg). Thereafter, the trachea was exposed using fine dissection scissors and a mid-cervical tracheotomy was performed by inserting a 20-gauge polyethylene catheter that was coupled to a flexiVent small animal ventilator (Scireq Inc. Montreal, PQ). Mice were ventilated with a tidal volume of 10 ml/kg body weight, 150 times per minute with an inspiration:expiration time ratio of 1:1.5. A positive end expiratory pressure (PEEP) of 3 cmH_2O, achieved by submerging the expiratory outlet from the ventilator into a water trap, was used for all studies. Once equilibrated on the ventilator, mice were subjected to a serial aerosol methacholine (MCh)

challenge protocol to assess concentration response characteristics of respiratory mechanics. Prior to delivery of each concentration of MCh, the loading history of the lung was normalized by inflating to total lung capacity and then allowing deflation to functional residual capacity. For MCh challenge, ~ 30μL of saline containing from 0 to 50 mg/ml MCh was delivered over 10 seconds using an in-line ultrasonic nebulizer. Measurement of respiratory mechanics in response to each dose of MCh was initiated within 10 seconds of completing the aerosol MCh challenge, with total measurement duration of 5 minutes thereafter. After challenge and the measurement period for each MCh concentration, the next highest concentration of MCh was administered until the maximum concentration was attained.

To assess the effects of MCh challenge on respiratory mechanics we used a low frequency forced oscillation technique in which mechanical ventilation was interrupted, then a volume perturbation signal was applied using a preset flexiVent Prime-8 protocol. The 8 second perturbation signal consisted of 18 serial sine waves spanning a frequency range of 0.25 Hz to 19.625 Hz. In total, 20 perturbations were completed during the course of each 5-minute measurement period. Respiratory mechanical input impedance (*Zrs*) was derived from the displacement of the ventilator's piston and the pressure in its cylinder. Correction for gas compressibility, and resistive and accelerative losses in ventilator, tubing and catheter were performed according manufacturer instructions, using dynamic calibration data obtained from volume perturbations applied to the system in an open and closed configuration. By fitting *Zrs* to the constant phase model, flexiVENT software calculated conducting airway resistance (Rn), peripheral tissue and airway resistance (G) and tissue elastance or stiffness (H); each parameter was normalized according to body weight. Values for each parameter were calculated as the mean of all 20 perturbation cycles performed after each MCh challenge.

To assess the effects of inhibiting ROCK1/2 on baseline respiratory mechanics, a separate cohort of mice were anesthetized 30 minutes after exposure to aerosolized Y-27632 (5 mM for 5min) [81] with an intra-peritoneal injection of sodium pentobarbital (60 mg/kg). Following anesthesia, respiratory mechanics were performed as previously described in detail above.

Lung Morphometry

Histology and morphometric assessment were performed using the left lung. Lungs were removed from the mice and inflated with 10% buffered formalin to a pressure of 25 cm H_2O, and fixed for 24 hours prior to further processing. After fixation, the left lung was separated into equal halves with a single mid-line cut in cross section; the lower (posterior) half of the lung was embedded in paraffin for subsequent preparation of serial lung cross sections (6μm) that were used to analyze large bronchi; the upper (anterior) half of the lung was cut longitudinally just distal to the central mainstem bronchus, and was then embedded for subsequent preparation of serial longitudinal lung sections (6 μm) for analysis of sub-segmental peripheral airways.

For quantitative morphometry, smooth muscle in tissue sections was labeled colorimetrically with mouse anti-sm-α-actin antibodies (Clone 1A4, Dako, Denmark), using the streptavidin-biotin complex method with 3, 3'-diaminobenzidine substrate and 100 μl of hydrogen peroxidase in 50 mM Tris-HCl, pH 7.6. Collagen was stained using picro sirius red and was visualized by microscopy under a polarizing filter. For general assessment of morphology, tissues were also stained using standard hematoxylin eosin. Specimens were viewed using an upright light microscope equipped with SPOT CCD camera and ImagePro (Olympus Canada) imaging software. Specific airways and regions of airway wall were selected for analysis using the criteria described by Hirota et. al.[82]; these included: 1) airways were intact and completely

included in the field of view, 2) the ratio of maximum diameter/minimum diameter was ≤ 2 to avoid artifacts from airways cut transversely, and (c) areas used for quantification were not spatially associated with nearby arteries. Central airways in cross sections of posterior left lung were grouped for analyses of "large airways". Basement membrane length was measured for all peripheral airways in longitudinal lung sections; the airways that were smaller than the mean of all peripheral airways were grouped together as "small airways" for subsequent analyses, whereas airways that had a BM length greater than the mean were grouped together as "medium airways".

For morphometry, a 35μm wide band extending from the basement membrane to the parenchyma was drawn, using a maximum length that adhered to selection criteria listed above. Quantitation modules in Image Pro (Olympus) software was used to measure sm-α-actin and picro sirius red staining within each band of interest; these measures were expressed as % positive staining, and reflected an integrated value based on intensity of staining and the total number of pixels that showed staining above a background threshold determined for each image. For all analyses, images of different airways were captured from 3-4 sections from each animal, and 5 animals were used in each group.

BALF and blood collection and analyses

Following the measurement of respiratory mechanics, the mice were removed from the ventilator with the catheter in place. The mice were lavaged with 500μL of cold saline, twice, for a total of 1mL. Blood was also collected after ventilation via cardiac puncture and serum was isolated for enzyme linked immunosorbent assays (ELISA). The collected bronchoalveolar lavage fluid (BALF) was centrifuged at 1500 rpm for 10 minutes. The supernatant was removed and used for

ELISA, while the pellet was resuspended in 500µL of ice cold saline. Total cell counts from the resuspended pellet were estimated using a hemocytometer then samples were diluted to a density of 400,000 cells/mL. Cells were spread onto slides using a Cytospin® 3 (Shandon Inc.) at 1000 rpm for 5 minutes. Thereafter, cells were stained with a modified Wright-Giemsa stain (Hema 3® Stat Pack, Fisher Scientific Co; catalogue #123-869). For cell differential analyses, six randomly chosen fields were examined under 40x magnification using an Olympus light microscope. Macrophages, lymphocytes, eosinophils and neutrophils were counted independently by two people in each field of view and were identified by cell morphology. Cell counts were totaled across the six fields of view and expressed as cells/mL of original BALF fluid.

ELISA

Our ELISA protocols have been reported in detail previously [83-84]. Bronchoalveolar lavage fluids were not diluted, but blood serum samples were diluted 1:10 in PBST for assay. In order to increase the specificity of the ELISA for IgE, total IgE in the samples was captured using goat anti-mouse IgE (2 mg/ml) and then the OVA-specific antibody was detected by use of biotinylated OVA [84]. Similar procedures were followed to increase the specificity of the ELISA for the remaining immunoglobulins of interest (IgG1, IgG2a, IgA). Data is expressed as relative immunoglobin levels using optical density (OD405) units.

Isometric force measurements of isolated tracheal rings

Female Cav-$1^{-/-}$ and B6129SF2/J mice were euthanized with 100µL of Somnitol (MTC Pharmaceuticals, Hamilton, ON). Tracheas were removed and dissected free of any surrounding connective tissue in Krebs-Henseleit (KH) buffer without Ca^{2+} (composition in mM: NaCl 112.6,

$NaHCO_3$ 25, NaH_2PO_4 1.38, KCl 4.7, $MgSO_4$ 2.46, Dextrose 5.56). Tracheas were then cut into 4 segments each containing three cartilage rings with intact smooth muscle and epithelium for subsequent measurement of contractile responses *ex vivo*. Tracheal smooth muscle reactivity was recorded using a temperature controlled (37°C) myograph (Multi Wire Model 610M, Danish Myo Technology, Aarhus, Denmark). Tissue preparations were submerged in Krebs-Henseleit buffer (composition in mM: NaCl 112.6, $NaHCO_3$ 25, NaH_2PO_4 1.38, KCl 4.7, $MgSO_4$ 2.46, Dextrose 5.56, $CaCl_2$ 2.5). The solution was constantly aerated with a 5% CO_2 / 95% room air mixture to maintain a pH of 7.4. Each tracheal ring preparation was mounted between two wire pins; one pin was linked to the isometric force transducer and the other pin's position could be adjusted using an attached micrometer to alter the resting load on the muscle. Each trachea was positioned on the pins so that the muscle was oriented in parallel with the force transducer. Following the initial mounting, each tracheal preparation was left to equilibrate for 1 hour under zero tension. Thereafter, as has been described for other studies [85], the resting tension required for maximum force generation of each preparation was determined. Briefly, segments were initially loaded with 0.3mN tension and following a 5 minute equilibration period, contraction was induced with an iso-osmotic KH solution containing 50mM KCl (composition in mM: KCl 50, NaCl 73.1, $NaHCO_3$ 25, NaH_2PO_4 1.38, $MgSO_4$ 2.46, Dextrose 5.56, $CaCl_2$ 2.5). When maximal contraction was reached after each KCl stimulation, the preparations were washed twice with normal KH solution and left to rest for 5 min. This procedure was repeated until the increase in load did not cause an increase in maximum isometric force. Thereafter, preparations were incubated with 3μM indomethacin (Sigma Chemicals, St. Louis) for 30 minutes to inhibit epithelial prostaglandin release. Following the 30 minute incubation with indomethacin, cumulative concentration-response curves for methacholine (Sigma Chemicals, St. Louis) were

measured. For all experiments, methacholine-induced contractions of individual preparations were normalized to the maximum KCl-induced contraction in order to account for any differences in the size of the preparations.

Once the above measurements were made, an additional series of experiments were performed to identify signaling pathways involved in the contractile pathways in Cav-$1^{-/-}$ and B6129SF2/J mice. Tracheas were prepared and mounted onto the myograph in the same manner as described above. They were left to equilibrate for 1 hour under zero tension and then resting tension was determined using the same procedures as described above. Preparations remained at the optimal tension and were incubated with 3μM indomethacin for 30 minutes before the administration of methacholine to inhibit epithelial prostaglandin release. In addition, inhibitors for Rho kinase (1μM and 10μM Y-27632), PKC (3μM GF 109203X aka bisindolylmaleimide) or an upstream inhibitor of ERK1/2 (3μM U0126) were added in 30 minutes prior to methacholine stimulation. The concentration of each inhibitor used in this study represents the one that produced a maximal inhibition without suppressing contraction completely in pilot studies using BALB/c mice. Following the 30 minute incubation with indomethacin, cumulative concentration-response curves for methacholine were measured. During analysis, methacholine-induced contractions of individual preparations were normalized to their KCl-induced contraction in order to account for any differences in the size of the preparations.

Statistical Analysis

All results are expressed as mean ± S.E., where *n* equals the number of animals used. The methacholine concentration response curves were fitted to a sigmoidal dose response curve with variable slope to determine EC50 values (GraphPad Prism 4). Curves were compared with an F-

test. Statistical analysis was performed using Student's unpaired two-tailed t-test and one-way analysis of variance with Tukey-Kramer post-hoc test where appropriate. A p value of <0.05 was considered significant.

VI. Results

Abundance of caveolin proteins and caveolae in Cav-1$^{-/-}$ mice.

To confirm the phenotype of Cav-1$^{-/-}$ mice, we first used immunoblotting and RT-PCR to assess caveolin mRNA and protein in tissues isolated from Cav-1$^{-/-}$ mice and the recommended genetic control strain, B6129SF2/J. By PCR we were able to detect mRNA for caveolin-2 and caveolin-3 in all of the tissues examined from B6129SF2/J and Cav-1$^{-/-}$ mice, whereas as expected, Cav-1 mRNA was absent in all tissues from Cav-1$^{-/-}$ mice (Figure 4A). Similarly,

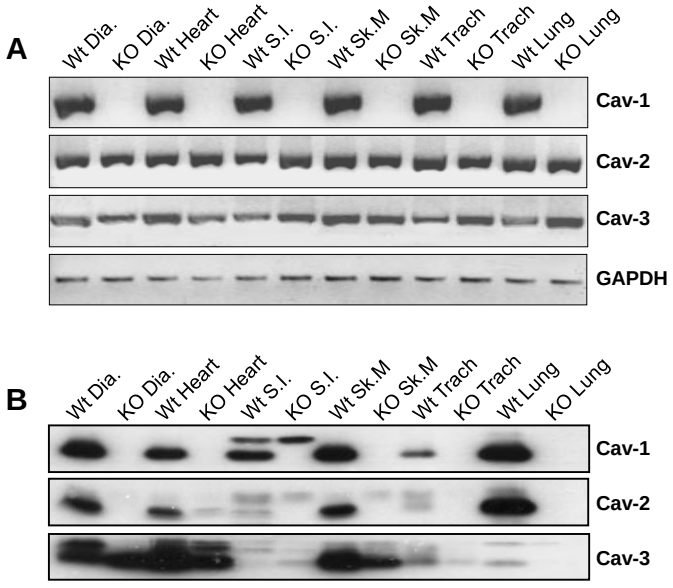

Figure 4- Expression of caveolins in isolated tissue from caveolin-1 knockout mice (KO) and B6129SF2/J mice (WT). (A) RT- PCR demonstrating an absence of caveolin-1 mRNA in diaphragm (Dia), heart, small intestine (S.I), skeletal muscle (Sk. M), trachea (Trach) and lung isolated from caveolin-1 knockout mice. Normal expression is seen in the same tissues isolated from B6129SF2/J mice. Caveolin-2 and caveolin-3 expression was similar between mouse strains **(B)** Immunoblot demonstrating an absence of caveolin-1 protein expression in tissues isolated from caveolin-1 knockout mice. Caveolin-2 protein expression was also reduced in tissue isolated from knockout mice when compared with tissues isolated from B6129SF2/J mice.

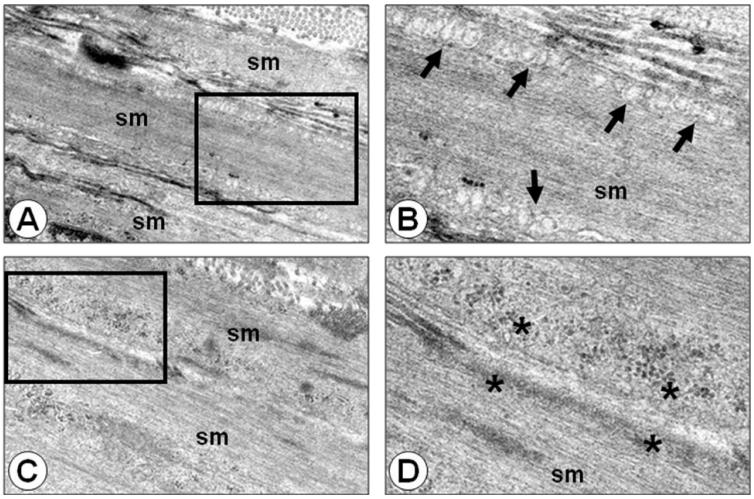

Figure 5- Electron micrograph of airway smooth muscle cells (sm) from the central airways of caveolin-1 knockout mice (C and D) and B6129SF2/J mice (A and B). Caveolae are visible along the smooth muscle cell membranes from B6129SF2/J mice (shown by arrows in B); however, these structures are absent in similar smooth muscle cell membranes from caveolin-1 knockout mice (absence demonstrated by * in D).

immunoblotting confirmed a lack of Cav-1 protein in the diaphragm, heart, small intestine, skeletal muscle, lungs and trachea of the Cav-$1^{-/-}$ mice (Figure 4B). Caveolin-2 protein abundance was reduced dramatically in most tissues, including the lungs, whereas caveolin-3 abundance was not different between knock out and wild type mouse strains (Figure 4B). To further assess the phenotype of smooth muscle cells in the central airways of Cav-$1^{-/-}$ mice, we also assessed ultrastructure using transmission electron microscopy (Figure 5). Though caveolae were readily detectable and abundant in airway smooth muscle cells of B6129SF2/J mice (Figure 5 A&B), caveolae were not visible in the airway smooth muscle layer from Cav-$1^{-/-}$ mice (Figure 5 C&D). As a final assessment of lung phenotype in Cav-$1^{-/-}$ mice, we also assessed the organization of the peripheral lung by histochemistry with hemotoxylin and eosin staining (Figure 6A). Consistent with previous reports [31-32, 38], we observed thickened alveolar septae, and reduced alveolar spaces containing extravasated red blood cells. Collectively, these

data confirm that the Cav-1$^{-/-}$ mice we studied exhibit lung remodeling that is consistent with the descriptions published by other groups.

Effect of Cav-1$^{-/-}$ on Respiratory Mechanics in vivo

Though our observations confirm previous reports for an altered lung phenotype in Cav-1$^{-/-}$ mice, to date there has been limited reports of the effects these changes have on the function of the respiratory system. Therefore, we measured respiratory mechanics in Cav-1$^{-/-}$ and B6129SF2/J mice using low frequency forced oscillation with a *flexi*VENT (Scireq, Montreal, PQ) small animal ventilator. Though Cav-1$^{-/-}$ mice have a mixed genetic background mimicked by B6129SF2/J mice, there are no reports describing baseline lung mechanics in the latter strain. However, the genetic background of both Cav-1$^{-/-}$ and B6129SF2/J mice include a significant (>50%) contribution from C57BL/6 mice. C57BL/6 mice have been used frequently to assess lung mechanics and are known to exhibit relative low responsiveness to inhaled methacholine [86-88]. Thus, for all studies of respiratory mechanics we also included C57BL/6 mice as a control to ensure that any differences between Cav-1$^{-/-}$ and B6129SF2/J mice were due to Cav-1 deficiency and were not an indirect consequence of C57BL/6-derived hyporesponsiveness. To assess lung function and airway responsiveness, we measured changes in respiratory mechanics that occurred during aerosol challenge with 0-50mg/mL of the bronchospastic agent, methacholine.

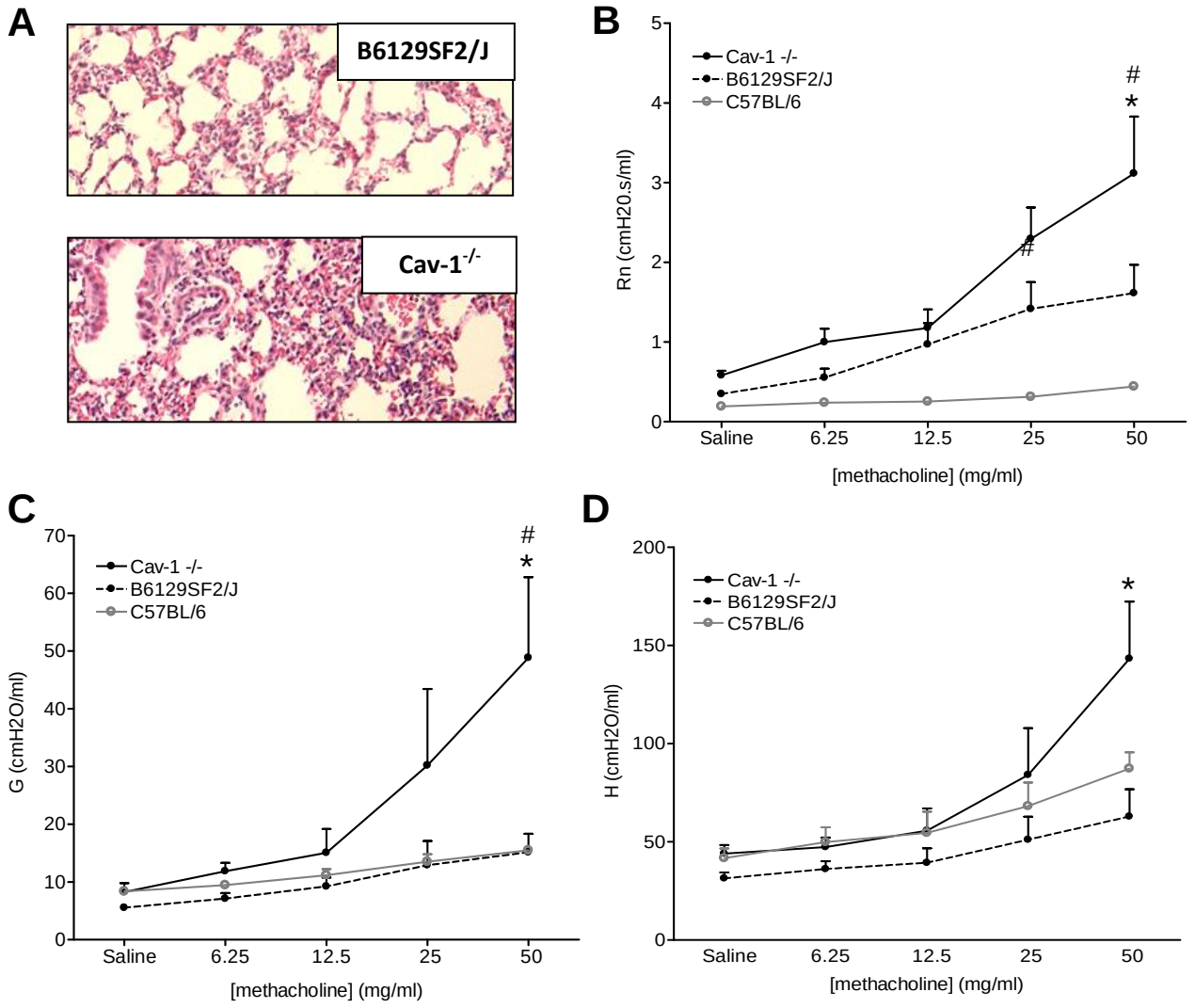

Figure 6- Respiratory Mechanics of caveolin-1 knockout (Cav-1 $^{-/-}$), B6129SF2/J and C57BL/6 mice. (A) Hemotoxylin and eosin staining of lung parenchyma from Cav-1$^{-/-}$ and B6129SF2/J mice. Parenchyma from Cav-1$^{-/-}$ mice demonstrate thickened alveolar septae and reduced alveolar spaces containing extravasated red blood cells. **(B)** Comparison of airway resistance (Rn) between Cav-1$^{-/-}$, B6129SF2/J and C57BL/6 mice with increasing doses of inhaled methacholine. Cav-1$^{-/-}$ mice demonstrate significantly heightened airway resistance compared to C57BL/6 mice at 25 mg/ml and 50 mg/ml methacholine (# $p<0.05$). In addition, airway resistance in Cav-1$^{-/-}$ mice is significantly greater than airway resistance in B6129SF2/J mice at 50 mg/ml methacholine (*$p<0.05$). **(C)** Comparison of tissue damping (G) between Cav-1$^{-/-}$, B6129SF2/J and C57BL/6 mice with increasing doses of inhaled methacholine. Cav-1$^{-/-}$ mice demonstrate significantly heightened tissue damping compared to C57BL/6 mice (#$p<0.05$) and B6129SF2/J mice (*$p<0.05$) at 50 mg/ml methacholine. **(D)** Comparison of tissue elastance (H) between Cav-1$^{-/-}$, B6129SF2/J and C57BL/6 mice with increasing doses of inhaled methacholine. Cav-1$^{-/-}$ mice demonstrate significantly heightened tissue elastance compared to B6129SF2/J mice at 50 mg/ml methacholine (*$p<0.05$).

After an initial saline inhalation, there were no significant differences in baseline central airway resistance (Rn) (Cav-1$^{-/-}$ 0.58 ± 0.06 cmH2O.s/ml, B6129SF2/J 0.35 ± 0.03 cmH2O.s/ml,

C57BL/6 0.19 ± 0.03 cmH2O.s/ml; p>0.05), tissue damping (G) (Cav-$1^{-/-}$ 8.25 ± 1.55 cmH2O/ml, B6129SF2/J 5.53 ± 0.51 cmH2O/ml, C57BL/6 8.36 ± 0.3 cmH2O/ml; p>0.05) and tissue elastance (H) (Cav-$1^{-/-}$ 44.00 ± 4.35 cmH2O.s/ml, B6129SF2/J 31.37 ± 3.04 cmH2O.s/ml, C57BL/6 41.68 ± 4.97 cmH2O.s/ml; p>0.05) between mouse strains (Figure 6). As previously described, C57BL/6 animals were relatively non-responsive to methacholine [86-87].

In contrast, after methacholine inhalation, Cav-$1^{-/-}$ mice after exhibited significantly greater increases in central airway resistance, compared to B6129SF2/J and C57BL/6 animals. Indeed, central airway resistance (Rn) in Cav-$1^{-/-}$ was double that measured for B6129SF2/J mice after inhalation of 50mg/ml methacholine (Cav-$1^{-/-}$ 3.12 ± 0.71 cmH2O.s/ml, B6129SF2/J 1.61 ± 0.36 cmH2O.s/ml; p<0.05) and 7 times that recorded for C57BL/6 mice (0.44 ± 0.05; p<0.05) (Figure 6B). Cav-$1^{-/-}$ mice also demonstrated enhanced tissue damping (G); a measure of the energy dissipation in the lung tissue that is in part a determinant of peripheral airway resistance and alveolar de-recruitment. More specifically, tissue damping was 3 times higher in Cav-$1^{-/-}$ mice after the inhalation of 50mg/ml methacholine compared to both C57BL/6 and B6129SF2/J mice (Cav-$1^{-/-}$ 48.82 ± 13.95 cmH2O/ml, B6129SF2/J 15.15 ± 3.20 cmH2O/ml, C57BL/6 15.48 ± 0.25 cmH2O/ml; p<0.05) (Figure 6C). Tissue elastance (H) was also significantly heightened in Cav-$1^{-/-}$ mice compared to B6129SF2/J (Cav-$1^{-/-}$ 143.31 ± 29.01 cmH2O/ml, B6129SF2/J 62.92 ± 13.86 cmH2O/ml; p<0.05); whereas no significant difference was measured in comparison to C57BL/6 mice, though a trend for increased elastance was certainly evident (C57BL/6 87.37 ± 8.24cmH2O/ml; p>0.05 compared to Cav-$1^{-/-}$) (Figure 6D). Collectively, these data suggest that, compared to B6129SF2/J and C57BL/6 mice, airways from Cav-$1^{-/-}$ mice likely possess intrinsic differences that contribute to greater narrowing when challenged with methacholine. Moreover, the altered peripheral lung phenotype we and others have observed in Cav-$1^{-/-}$ mice appears to

correlate with increased maximum stiffness and tissue resistance in response to inhaled methacholine.

Table 1- Average basement membrane length of airways from caveolin-1 knockout (Cav-1$^{-/-}$) and B6129SF2/J mice

	Large central airways	Medium peripheral airways	Small peripheral airways
Cav-1$^{-/-}$	990.35 ± 89.60 μm	947.44 ± 32.01 μm	583.34 ± 16.98 μm
B6129SF2/J	1077.69 ± 67.22 μm	847.11 ± 21.76 μm	572.32 ± 22.38 μm

Morphometrical analysis of the structural differences in Cav-1$^{-/-}$ mice.

Since structural differences of the central and peripheral airways of the Cav-1$^{-/-}$ mice could account for increased airway and tissue resistance respectively, we next performed quantitative morphometric analyses of the airways to measure both collagen abundance and contractile tissue mass. Lungs from Cav-1$^{-/-}$ and B6129SF2/J mice were sectioned and stained with Picrosirius Red to measure collagen abundance. In addition, lung sections from both mouse strains were stained for smooth muscle (sm)-α-actin using immunohistochemistry techniques to quantify the abundance of contractile tissue mass. In order to fully characterize the differences in structure contributing to the increased resistance observed *in vivo* (Rn and G), airways were subdivided into large (central) airways and small and medium peripheral airways for making comparisons between strains. Average basement membrane length for each group of airways was not different between Cav-1$^{-/-}$ and B6129SF2/J mice (Table 1).

Cav-1$^{-/-}$ mice exhibited marked collagen staining surrounding central and peripheral airways (Figure 7). Positive staining for collagen was over 15 times greater in large central airways of Cav-1$^{-/-}$ (7.33 ± 1.72%) compared to B6129SF2/J mice (0.43 ± 0.21%; $p<0.015$). Similar trends were seen in medium sized and small peripheral airways where collagen staining was 3 times

higher in Cav-1$^{-/-}$ mice (Medium sized airways: Cav-1$^{-/-}$ 3.90 ± 1.55%, B6129SF2/J 1.20 ± 0.48%; $p<0.003$; small sized airways: Cav-1$^{-/-}$ 2.16 ± 0.62%, B6129SF2/J 0.70 ± 0.31%; $p<0.009$). Collectively, these data indicate that airways of Cav-1$^{-/-}$ mice are marked by significant fibrosis that contributes to increased wall thickness.

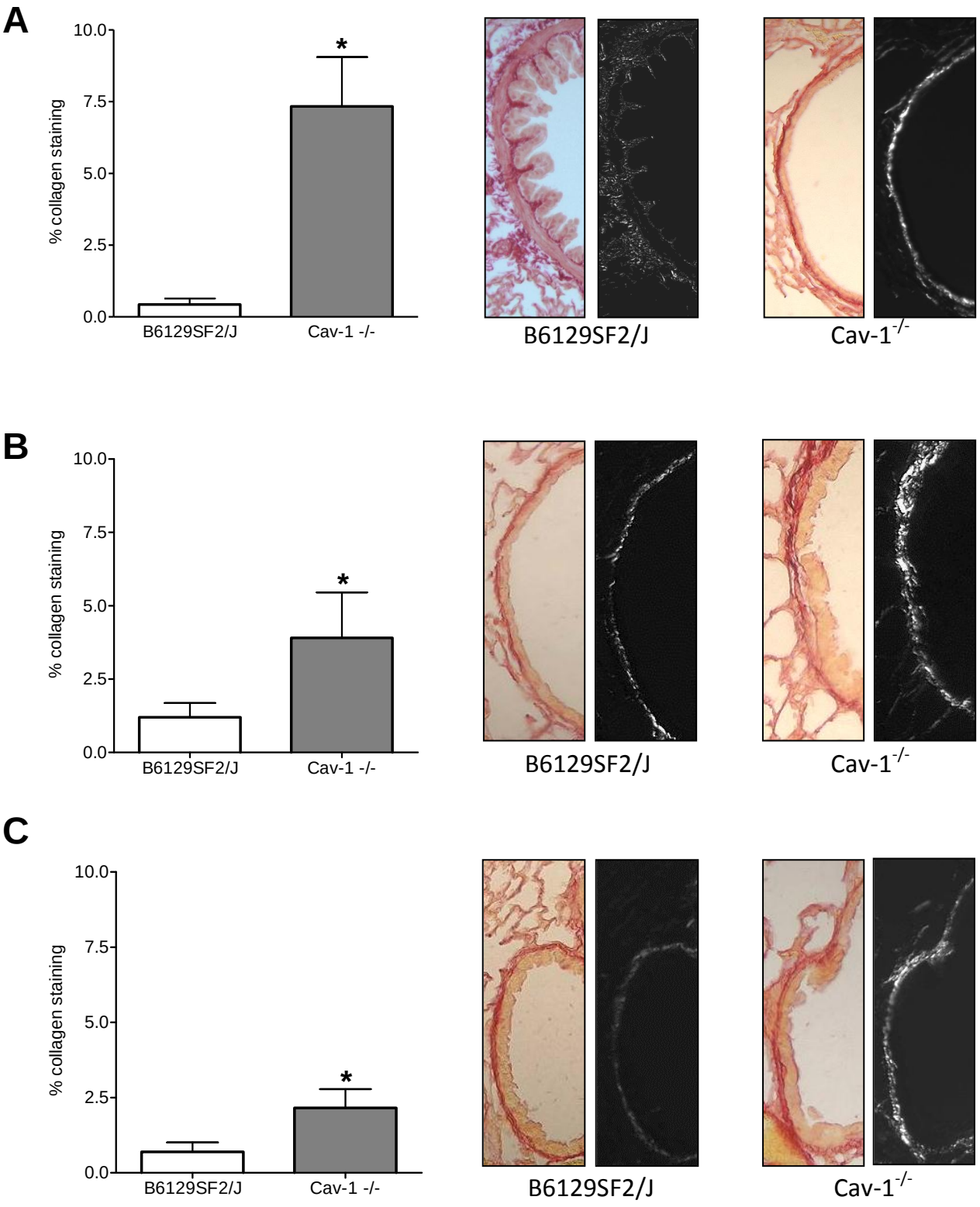

Figure 7- Comparison of collagen abundance in large (A), medium (B) and small (C) airways in caveolin-1 knockout (Cav-1$^{-/-}$) and B6129SF2/J mice. Positive staining of collagen with picrosirius red is shown under light microscopy in red (left) and with a polarizing filter in white (right) for each airway size. Cav-1$^{-/-}$ mice have significantly greater picrosirius red staining of collagen in **(A)** large airways (*p<0.015), **(B)** medium airways (*p<0.003) and **(C)** small airways (*p<0.009) compared to B6129SF2/J.

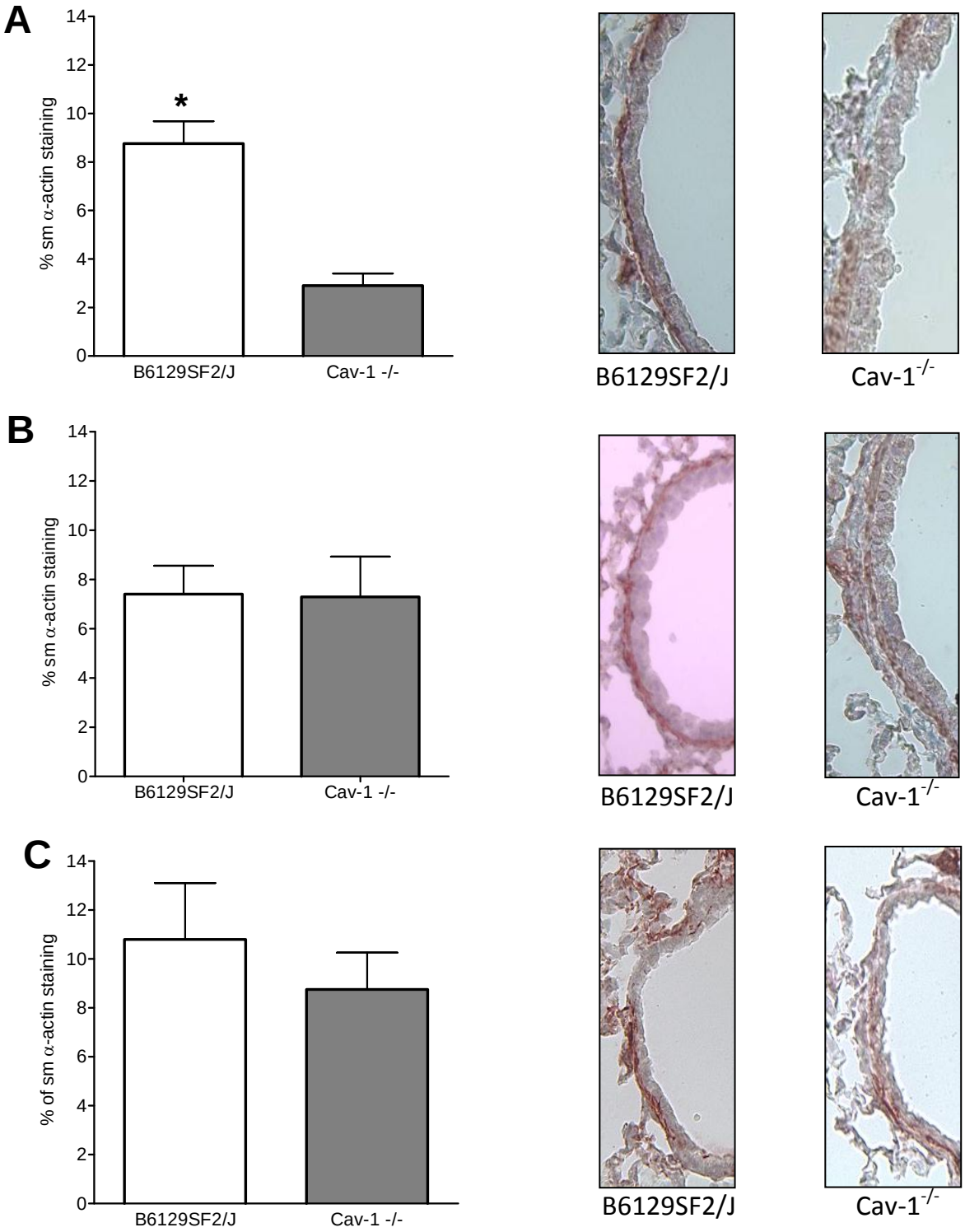

Figure 8- Comparison of airway smooth muscle α-actin abundance in large (A), medium (B) and small (C) airways in caveolin-1 knockout (Cav-1$^{-/-}$) and B6129SF2/J mice. Positive staining of smooth muscle α-actin by immunohistochemistry is shown under light microscopy for each airway size. B6129SF2/J mice exhibited significantly more smooth muscle α-actin staining in large airways compared to Cav-1$^{-/-}$ mice (*$p<0.05$). There was no significant difference in the abundance of airway smooth muscle α-actin in medium airways **(B)** and small airways **(C)** of both mouse strains.

In contrast to differences we observed in collagen abundance, morphometric analyses of the airways revealed no significant difference in sm-α-actin tissue surrounding small (Cav-$1^{-/-}$ 8.75 ± 1.51%, B6129SF2/J 10.80 ± 2.30%; $p>0.05$) or medium sized peripheral airways (Cav-$1^{-/-}$ 7.29 ± 1.64%, B6129SF2/J 7.41 ± 1.15%; $p>0.05$) between Cav-$1^{-/-}$ and B6129SF2/J mice (Figure 8). Conversely, sm-α-actin positive area was twofold higher in the central airways of B6129SF2/J animals compared to Cav-$1^{-/-}$ mice (Cav-$1^{-/-}$ 2.90 ± 0.50%, B6129SF2/J 8.76 ± 0.92%; $p<0.02$). Collectively, these data indicate that increased airway reactivity to methacholine in Cav-$1^{-/-}$ mice is not related to an increase in contractile tissue mass surrounding the airways. (Figure 6B,C).

Baseline airway inflammation in naïve Cav-$1^{-/-}$ mice

To better understand mechanisms that underpin airway fibrosis in naïve Cav-$1^{-/-}$ mice, we next quantified airway inflammation using bronchoalveolar lavage fluid (BALF) collected from Cav-$1^{-/-}$ and B6129SF2/J mice. Prior to BALF analyses we first confirmed that naïve Cav-$1^{-/-}$ mice did not exhibit an idiopathic allergic phenotype by comparing immunoglobin levels (IgG1, IgG2a and IgA) in serum from Cav-$1^{-/-}$ and B6129SF2/J mice (Figure 9A). No differences in the levels of immunoglobulins was seen between strains (IgG1: Cav-$1^{-/-}$ 0.14 ± 0.01 pg/ml, B6129SF2/J 0.14 ± 0.02 pg/ml; $p>0.05$, IgG2a: Cav-$1^{-/-}$ 0.12 ± 0.03 pg/ml, B6129SF2/J 0.16 ± 0.01 pg/ml; $p>0.05$, IgA: 0.078 ± 0.003 pg/ml, B6129SF2/J 0.077 ± 0.002 pg/ml; $p>0.05$).

To assess airway inflammation, we used enzyme-linked immunosorbent assays (ELISAs) and determined inflammatory cell count and differentials. We first assayed BALF for a panel of pro-inflammatory cytokines that included interleukin-5 (IL-5; a Th2 polarized eosinophil trophic factor), interferon gamma (IFNγ; a stereotypical Th1 class cytokine), tumor necrosis factor alpha (TNF-α; a pro-inflammatory cytokine linked to airway hyperresponsiveness (AHR), and

transforming growth factor beta (TGF-β1; a pro-fibrotic cytokine associated with asthma pathogenesis) (Figure 9B).

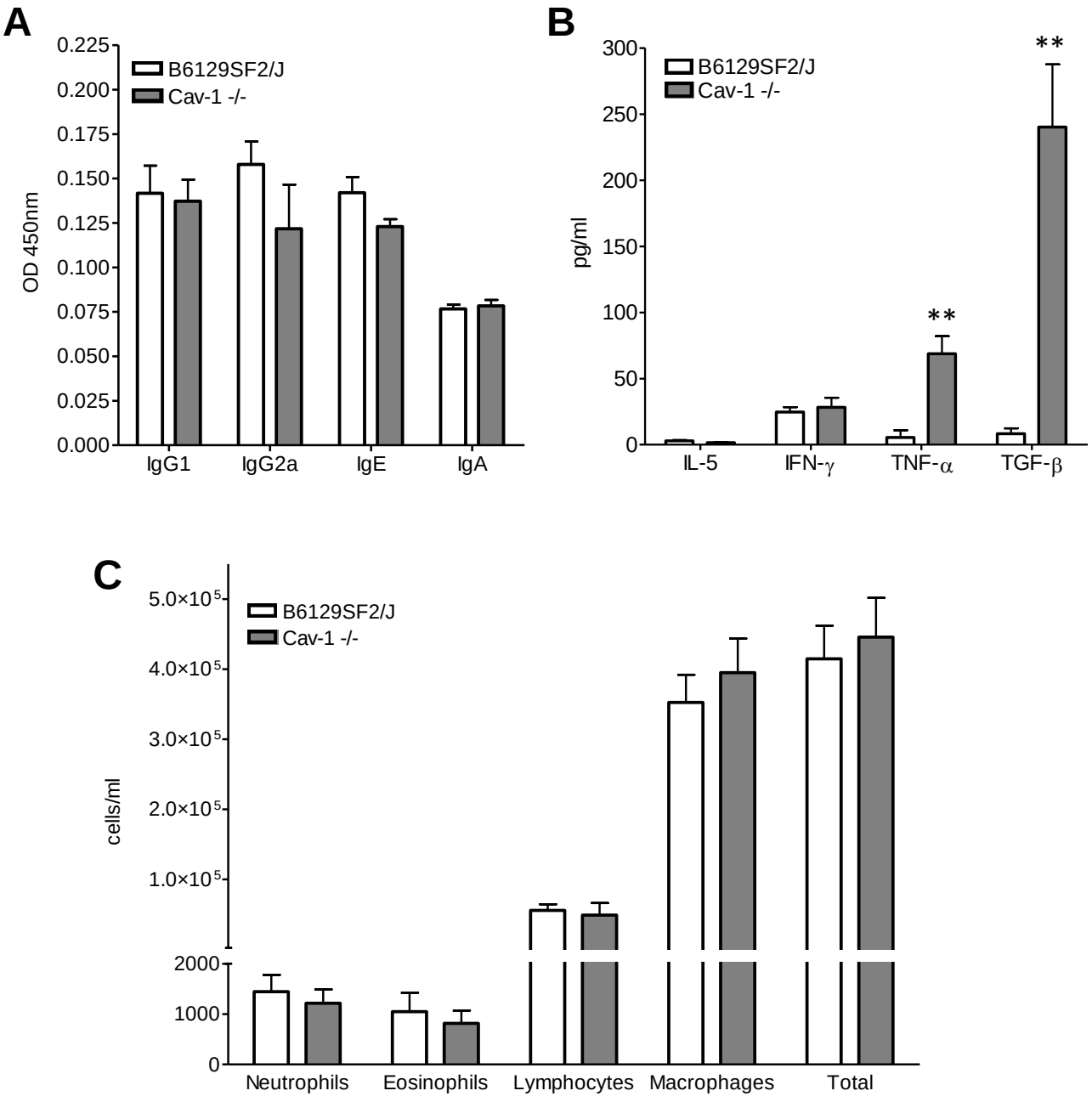

Figure 9- Comparison of the baseline inflammatory profile between caveolin-1 knockout mice (Cav-1$^{-/-}$) and B6129SF2/J mice. (A) Comparison of immunoglobulin (Ig) levels in the serum of Cav-1$^{-/-}$ and B6129SF2/J mice. There were no significant differences in serum levels of IgG1, IgG2a, IgE or IgA between mouse strains. **(B)** Comparison of pro-inflammatory cytokine levels in bronchoalveolar lavage fluid (BALF) from Cav-1$^{-/-}$ and

B6129SF2/J mice. Transforming growth factor β (TGF-β)(**p<0.01) levels and tumor necrosis factor α (TNF-α)(**p<0.01) levels were significantly greater in the BALF from Cav-$1^{-/-}$ mice compared with BALF from B6129SF2/J mice. Interleukin 5 (IL-5) and interferon γ (IFN-γ) levels did not differ significantly between mouse strains. **(C)** Differential inflammatory cell counts in BALF isolated from Cav-$1^{-/-}$ and B6129SF2/J mice. There were no significant differences in the total number of cells isolated from the BALF of Cav-$1^{-/-}$ and B6129SF2/J mice. In addition, there were no significant differences in the number of neutrophils, eosinophils, lymphocytes, or macrophages in BALF isolated from Cav-$1^{-/-}$ compared to BALF isolated from B6129SF2/J mice.

IL-5 and IFN-γ levels did not differ between mouse strains, suggesting there was no basal shift in the Th1/Th2 balance in Cav-$1^{-/-}$ mice (IL-5: Cav-$1^{-/-}$ 1.5 ± 0.43 pg/ml, B6129SF2/J 2.84 ± 0.70 pg/ml; p>0.05, IFN-γ: Cav-$1^{-/-}$ 28.23 ± 7.32 pg/ml, B6129SF2/J 24.65 ± 3.72 pg/ml, p>0.05). In contrast, BALF from Cav-$1^{-/-}$ contained markedly increased levels of both TGF-β (Cav-$1^{-/-}$ 240.20 ± 47.36, B6129SF2/J 8.35 ± 4.03 pg/ml; p<0.003) and TNF-α (Cav-$1^{-/-}$ 68.84 ± 13.25 pg/ml, B6129SF2/J 5.44 ± 5.44 pg/ml; p<0.004). To determine whether these changes in cytokine levels were linked with cellular inflammation, we next performed differential inflammatory cell counts using BALF to assess the relative abundance of eosinophils, neutrophils, lymphocytes and macrophages. The total number of inflammatory cells in the BALF did not differ between mouse strains (Cav-$1^{-/-}$ $4.5x10^5$ ± $1.1x10^5$ cells/ml, B6129SF2/J $4.1x10^5$ ± $1.3x10^5$ cells/ml; p>0.05) (Figure 9C). Moreover, there were no significant differences in the relative numbers of eosinophils (Cav-$1^{-/-}$ 817 ± 566 cells/ml, B6129SF2/J 1050 ± 748 cells/ml; p>0.05), neutrophils (Cav-$1^{-/-}$ 1214 ± 618 cells/ml, B6129SF2/J 1445 ± 752 cells/ml; p>0.05), lymphocytes (Cav-$1^{-/-}$ $4.9x10^4$ ± $3.9x10^4$ cells/ml, B6129SF2/J $5.6x10^4$ ± $2.0x10^4$ cells/ml; p>0.05) or macrophages (Cav-$1^{-/-}$ $4.0x10^5$ ± $1.1x10^5$ cells/ml, $3.5x10^5$ ± $8.8x10^4$ cells/ml; p>0.05). Collectively, the data reveal that the profibrotic cytokine TGFβ1 and AHR-linked cytokine TNF-α are elevated in BALF of Cav-$1^{-/-}$ mice, but this occurs in the absence of any increase in recruited inflammatory cells.

Contractile response of airway smooth muscle from Cav-1$^{-/-}$ mice

Our *in vivo* analyses revealed airway hyperreactivity to inhaled methacholine as a phenotypic feature of Cav-1$^{-/-}$ mice. As airway reactivity is acutely determined by airway smooth muscle contraction leading to airway narrowing, we next performed *ex vivo* analyses to directly compare methacholine induced contraction of tracheal ring preparations from Cav-1$^{-/-}$ and B6129SF2/J mice. Tracheal rings were isolated and mounted on an isometric wire myograph and cumulative concentration-response curves for methacholine were determined. As shown in Figure 10A, basal tone was similar in preparations from Cav-1$^{-/-}$ and B6129SF2/J mice and methacholine evoked increased isometric tension in a concentration dependent manner. Active force generated in response to 50mM KCl stimulation was used to normalize contractile response of individual preparations to methacholine and was not different between mouse strains. In addition, the mean optimal tension used was similar for preparation from both mouse strains (~8mN). There were no apparent differences between mouse strains in the sensitivity of the tracheal smooth muscle to methacholine stimulation as the logEC50 values for Cav-1$^{-/-}$ and B6129SF2/J mice were -6.751 ± 0.093 and -6.908 ± 0.1345, respectively ($p>0.05$). Although there were no differences in sensitivity to methacholine, maximal contraction (induced with 50mg/ml methacholine) of tracheal smooth muscle preparations from Cav-1$^{-/-}$ mice was approximately 30% greater than that measured for tracheal rings from B6129SF2/J mice (Cav-1$^{-/-}$ 166.81 ± 8.07%, B6129SF2/J 127.72 ± 8.36%; $p<0.002$). Further analyses indicated that the reactivity of the airway smooth muscle from Cav-1$^{-/-}$ mice was significantly greater than airway smooth muscle from B6129SF/J mice in response to methacholine concentrations above $1x10^{-6}$ M ($p<0.01$). To ensure that differences in maximum contractile force were not the result of changes in airway smooth muscle mass, after each experiment, tracheas were subjected to immunohistological analysis

using sm-α-actin staining. As shown in Figure 10B, we observed no difference in the area of sm-α-actin staining in trachea rings from Cav-$1^{-/-}$ and B6219SF/J mice.

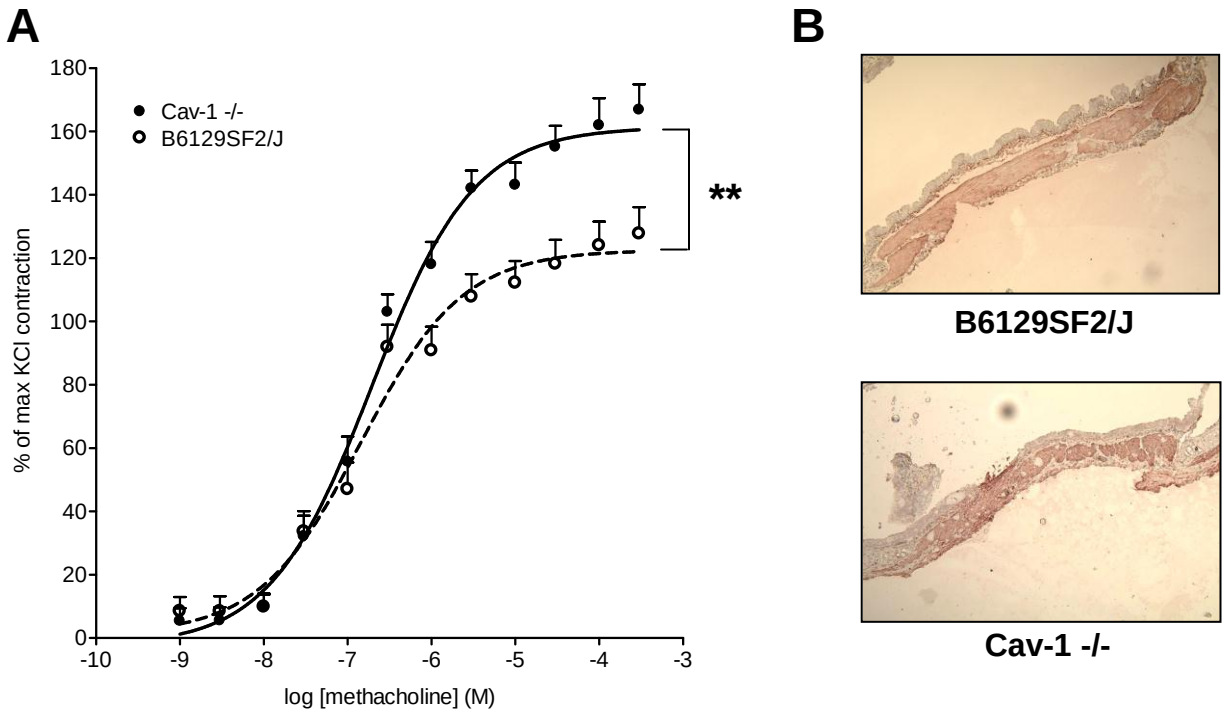

Figure 10- Assessment of airway (tracheal) smooth muscle contraction via myography. (A) Comparison of methacholine induced contraction of tracheal ring preparations from caveolin-1 knockout (Cav-$1^{-/-}$) and B6129SF2/J mice. Airway reactivity of tracheal smooth muscle from Cav-$1^{-/-}$ mice was significantly greater than reactivity of smooth muscle from B6129SF2/J mice at concentrations of methacholine greater than $1x10^{-6}$ M (-6)(**$p<0.01$). **(B)** Comparison of smooth muscle α-actin abundance in tracheas from Cav-$1^{-/-}$ and B6129SF2/J mice**.** Positive staining of smooth muscle α-actin by immunohistochemistry is shown under light microscopy for mouse strain. No significant difference in smooth muscle α-actin abundance was observed between mouse strains.

Collectively, these data suggest that Cav-$1^{-/-}$ mice exhibit enhanced airway reactivity to methacholine *ex vivo*. This observation is highly consistent with our studies *in vivo*, which demonstrated hyperreactivity of central airways and peripheral lung of Cav-$1^{-/-}$ mice to high concentrations of inhaled methacholine.

Effect of PKC inhibition on MCh-induced airway smooth muscle contraction

We sought to determine the pathway(s) underpinning the heightened airway smooth muscle contraction observed in the absence of Cav-1. Since Cav-1 has been implicated as a regulator of PKC dependent contractile pathways in both colonic and intestinal smooth muscle, we first performed experiments using a multi-wire myograph to determine if PKC signaling was the source of the hyperreactivity observed in Cav-$1^{-/-}$ mice. Tracheal rings were isolated from Cav-$1^{-/-}$ and B6129SF2/J mice and stimulated with increasing doses of methacholine in the presence and absence of the PKC inhibitor, GF 109203X, to asses any differences in the contractility of the airway smooth muscle. Prior to stimulation, basal tone was similar between mouse strains and KCl-induced contractions during the normalization procedure were comparable. As shown in figure 11 A and B, methacholine stimulation evoked isometric tension in a concentration dependent manner. Consistent with our previous findings, maximal contraction in tracheal smooth muscle from Cav-$1^{-/-}$ mice was heightened compared to muscle from B6129SF2/J mice (Figure 11C, Table 2). The hyperreactivity of the airway smooth muscle from Cav-$1^{-/-}$ mice was significant at doses of methacholine greater than $3x10^{-7}$ M ($p<0.05$). No significant differences in sensitivity to methacholine were observed between mouse strains (Table 2, pEC50 numbers). PKC inhibition had very little effect on the airway smooth muscle hyperreactivity observed in Cav-$1^{-/-}$ mice as maximal contraction and sensitivity toward methacholine were not affected by PKC inhibition (Figure 11C, Table 2). As shown in Table 2, maximal contraction in Cav-$1^{-/-}$ tracheal smooth muscle treated with GF 109203X remained heightened compared to muscle from B6129SF2/J mice. Taken collectively, these findings indicate that PKC signaling does not account for the airway smooth muscle hyperreactivity observed in Cav-$1^{-/-}$ mice.

Table 2. Contractile properties of tracheal preparations obtained from B6129SF2/J and Cav-1$^{-/-}$ mice

	B6129SF2/J		Cav-1$^{-/-}$	
	Emax	**pEC50**	**Emax**	**pEC50**
Control	128.56 ± 11.03	6.75 ± 0.12	230.26 ± 31.27**	6.71 ± 0.11
GF109203X (3μM)	119.01 ± 18.09	7.02 ± 0.06	210.10 ± 31.00 *	6.82 ± 0.06
Control	101.91 ± 9.03	6.51 ± 0.18	216.85 ± 27.40**	6.68 ± 0.15
U-0126 (3 μM)	100.18 ± 21.99	6.55 ± 0.36	185.58 ± 7.52**	6.71 ± 0.24
Control	135.29 ± 15.09	6.89 ± 0.12	186.73 ± 13.83*	6.92 ± 0.15
Y-27632 (1 μM)	127.96 ± 12.96	6.59 ± 0.02	164.45 ± 16.21	6.74 ± 0.33
Y-27632 (10 μM)	125.13 ± 4.64	6.37 ± 0.20$^{\#}$	121.07 ± 8.41$^{\#}$	6.61 ± 0.05

*Comparison of responses between Cav-1$^{-/-}$ and B6129SF2/J mice is statistically significant (*p<0.05).
**Comparison of responses between Cav-1$^{-/-}$ and B6129SF2/J mice is statistically significant (**p<0.001).
$^{\#}$ Comparison of responses between control and treatment groups within same mouse strain is significant ($^{\#}$p<0.05).

Effect of ERK1/2 inhibition on MCh-induced airway smooth muscle contraction

ERK1/2 activation can alter smooth muscle contraction via two Ca^{2+} independant mechanisms. Since Cav-1 is known to associate and potentially regulate ERK1/2 activity, we next performed myography experiments comparing the contractility of airway smooth muscle from Cav-1$^{-/-}$ and B6129SF2/J mice in the presence and absence of U0126, an upstream inhibitor of ERK1/2 signaling. As in the previous experiments, basal tone was comparable between mouse strains and there was no difference in contractile response to KCl stimulation during the normalization procedure.

In the absence of U0126, preparations isolated from Cav-1$^{-/-}$ mice exhibited heightened contractile force compared to preparations isolated from B6129SF2/J mice (Figure 12 A and B, Table 2). The hyperreactivity of the airway smooth muscle from Cav-1$^{-/-}$ mice was significant at doses of methacholine greater than 3x10-7 M ($p<0.05$). ERK1/2 inhibition had no effect on maximal-induced contraction or sensitivity to methacholine in preparations obtained from both mouse strains (Figure 12C, Table 2).

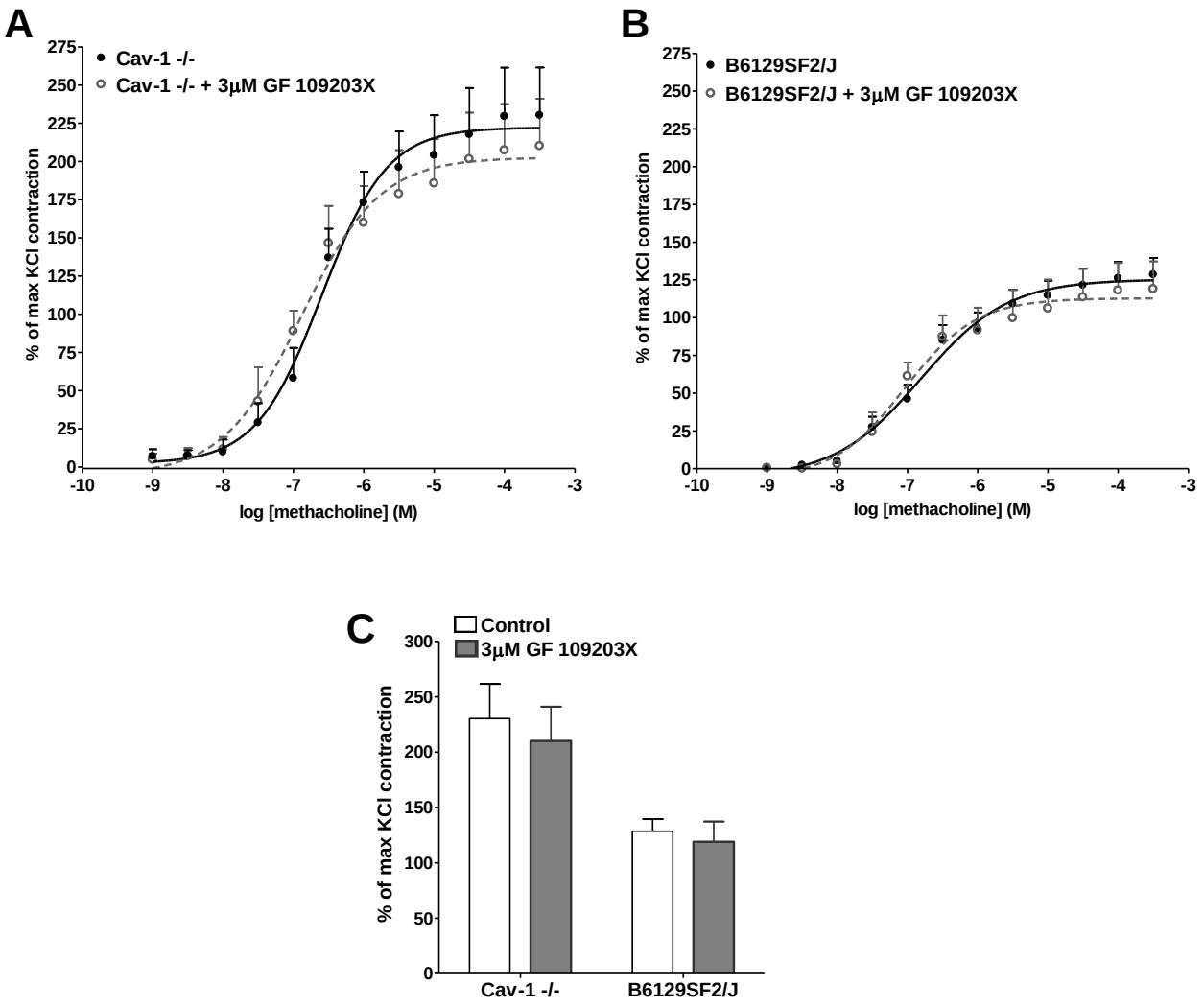

Figure 11: Effect of protein kinase C (PKC) inhibition on methacholine induced tracheal smooth muscle contraction. (A) Comparison of methacholine induced contraction of tracheal ring preparations from caveolin-1 knockout (Cav-$1^{-/-}$) mice with and without administration of 3µM of known PKC inhibitor – GF 109203X. **(B)** Comparison of methacholine induced contraction of tracheal ring preparations from B6129SF2/J mice with and without administration of 3µM of known PKC inhibitor – GF 109203X. **(C)** Comparison of responses to GF 109203X between mouse strains at maximum methacholine stimulation. Airway reactivity of tracheal smooth muscle from Cav-$1^{-/-}$ did not significantly differ with and without administration of GF 109203X ($p > 0.05$). Airway reactivity of tracheal smooth muscle from B6129SF2/J mice did not significantly differ with and without administration of GF 109203X ($p > 0.05$). Administration of GF 109203X did not normalize airway reactivity to methacholine between mouse strains. Tracheal smooth muscle preparations from Cav-$1^{-/-}$ mice remained hyperreactive compared with tracheal smooth muscle preparations from B6129SF2/J mice.

As shown in figure 12C and table 2, maximal contraction in Cav-$1^{-/-}$ tracheal smooth muscle treated with U0126 remained significantly heightened compared to muscle from B6129SF2/J mice.

In fact, airway smooth muscle contraction in tracheas from Cav-$1^{-/-}$ mice remained significantly higher than B6129SF2/J mice at methacholine doses greater than $3x10^{-6}$M even with U0126 treatment (Table 2, Figure 12 C). The data therefore suggests no role for ERK1/2 signaling in the augmented maximal methacholine-induced contraction in Cav-$1^{-/-}$ tracheal preparations.

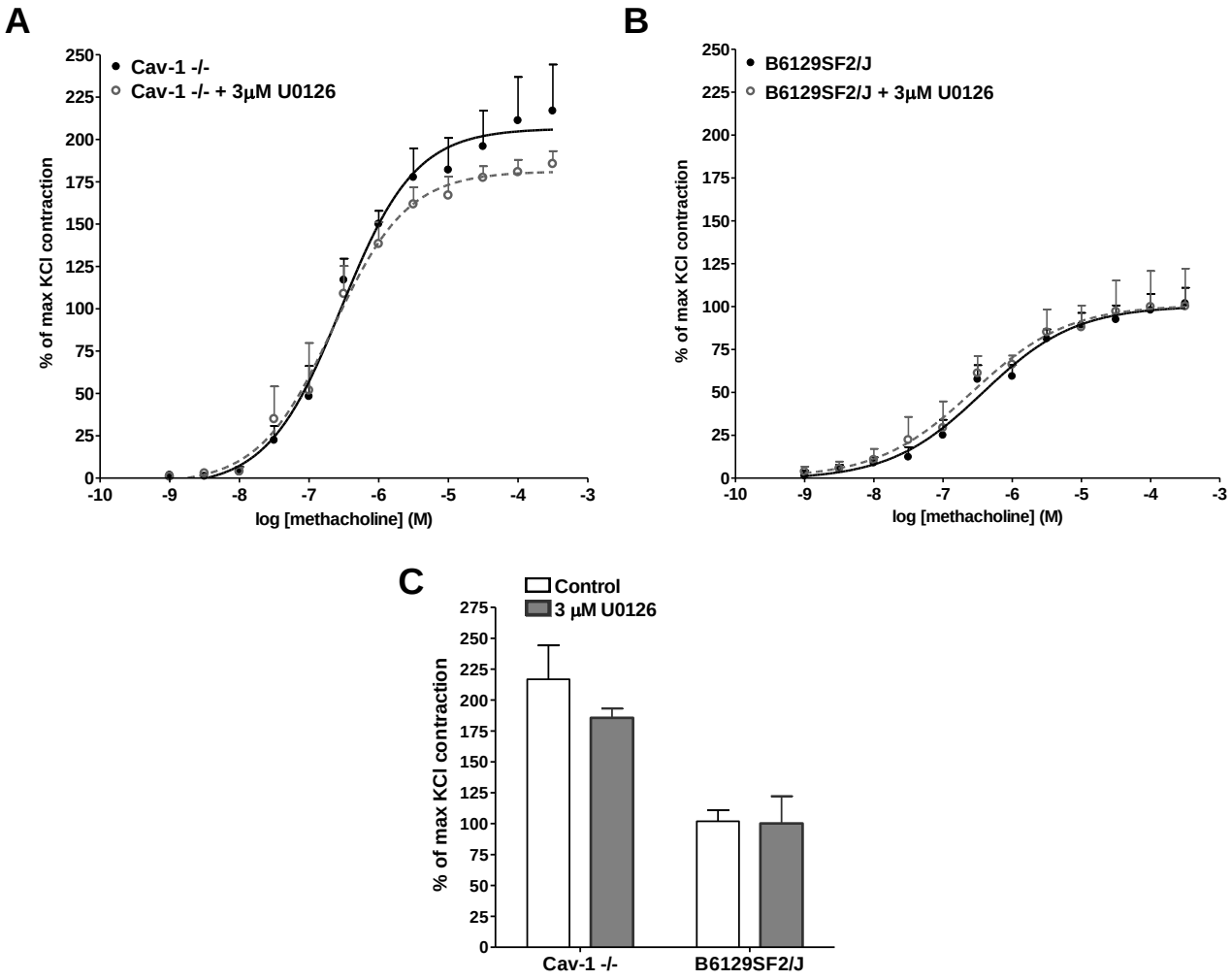

Figure 12: Effect of extracellular signal related kinase (ERK1/2) inhibition on methacholine induced tracheal smooth muscle contraction. (A) Comparison of methacholine induced contraction of tracheal ring preparations from caveolin-1 knockout (Cav-$1^{-/-}$) mice with and without administration of 3µM of known ERK1/2 inhibitor – U0126. **(B)** Comparison of methacholine induced contraction of tracheal ring preparations from B6129SF2/J mice with and without administration of 3µM of known ERK1/2 inhibitor – U0126. **(C)** Comparison of responses to U0126 between mouse strains at maximum methacholine stimulation. Airway reactivity of tracheal smooth muscle from Cav-$1^{-/-}$ did not significantly differ with and without administration of U0126 ($p > 0.05$). Airway reactivity of tracheal smooth muscle from B6129SF2/J mice did not significantly differ with and without administration of U0126 ($p > 0.05$). Administration of U0126 did not normalize airway reactivity to methacholine between mouse

strains. Tracheal smooth muscle preparations from Cav-$1^{-/-}$ mice remained hyperreactive compared with tracheal smooth muscle preparations from B6129SF2/J mice.

Effect of ROCK1/2 inhibition on MCh-induced airway smooth muscle contraction

Previous studies using vascular, colonic and intestinal smooth muscle demonstrate altered contraction via modulation of RhoA/ROCK1/2 signaling in the absence of Cav-1; however, the regulatory role of Cav-1 appears to depend on the muscle type. For example, in aged colonic smooth muscle, a reduction in Cav-1 expression results in the impairment of RhoA activation; whereas, in intestinal smooth muscle, the loss of Cav-1 causes an increase in Rho activation [37, 67]. To date, the interaction between Cav-1 and Rho/ROCK1/2 signaling has not been described in airway smooth muscle. Therefore, we sought to determine if enhanced RhoA/ROCK1/2 signaling was the source of the increased airway smooth muscle contraction observed in preparations from Cav-$1^{-/-}$ mice. We performed myography experiments in the presence of Y-27632, a selective ROCK1/2 inhibitor [81], and compared contractile responses between mouse strains. As observed in the previous experiments, basal tone and KCl-induced contractions were consistent between mouse strains during the normalization procedure.

In the absence of Y-27632, preparations from Cav-$1^{-/-}$ mice exhibited significantly heightened contractions compared to B6129SF2/J mice at methacholine doses greater than $3x10^{-6}$M ($p<0.05$) (Figure 13 A and B, Table 2). Pretreatment with 1μM Y-27632 did not affect maximal contraction or sensitivity towards methacholine in either mouse strain; instead, a trend for a rightward shift was observed in the B6129SF2/J mice. In contrast, increasing the pretreatment to 10μM Y-27632 reduced sensitivity and maximum response to MCh in both tissues, and even more importantly, completely normalized airway smooth muscle hypercontractility in

preparations from Cav-1$^{-/-}$ mice to levels of contraction comparable to maximal contraction in B6129SF2/J preparations. (Figure 13 C, Table 2).

Notably, whereas tracheas from Cav-1$^{-/-}$ exhibited concentration-dependent responses to Y-27632, there was no significant increase in suppression of contractile responses with 10μM compared to 1μM of inhibitor in B6129SF2/J mice (Figure 13 D). Furthermore, Y-27632 did not affect maximal contraction in B6129SF2/J preparations. Of note, no effect of 10 μM was observed on pEC50 in the Cav-1$^{-/-}$ preparations, whereas a significant reduction in sensitivity was observed in B6129SF2/J preparations. These data demonstrate that Rho kinase inhibition *ex vivo* is sufficient to inhibit airway smooth muscle hyperreactivity toward MCh in preparations from Cav-1$^{-/-}$ mice. Thus, the hyperreactivity observed in the airway smooth muscle from these mice is likely due to augmented ROCK1/2 signaling.

Effect of ROCK1/2 inhibition on Respiratory Mechanics in vivo

Our *in vivo* analyses revealed that Cav-1$^{-/-}$ mice demonstrate enhanced central and peripheral airway resistance, compared with B6129SF2/J mice, when exposed to inhaled methacholine. We further demonstrated that the enhanced airway resistance observed is likely due to hyperreactivity of airway smooth muscle from Cav-1$^{-/-}$ mice to methacholine. Interestingly, we demonstrated that this characteristic can be almost entirely reversed with inhibition of ROCK1/2 *ex vivo*. Thus, we were interested in determining if the altered respiratory mechanics observed in Cav-1$^{-/-}$ mice *in vivo* could also be normalized with the inhibition of this signaling pathway. As demonstrated previously, at baseline, Cav-1$^{-/-}$ mice exhibited significant airway hyperreactivity towards methacholine compared to B6129SF2/J controls (Figure 14).

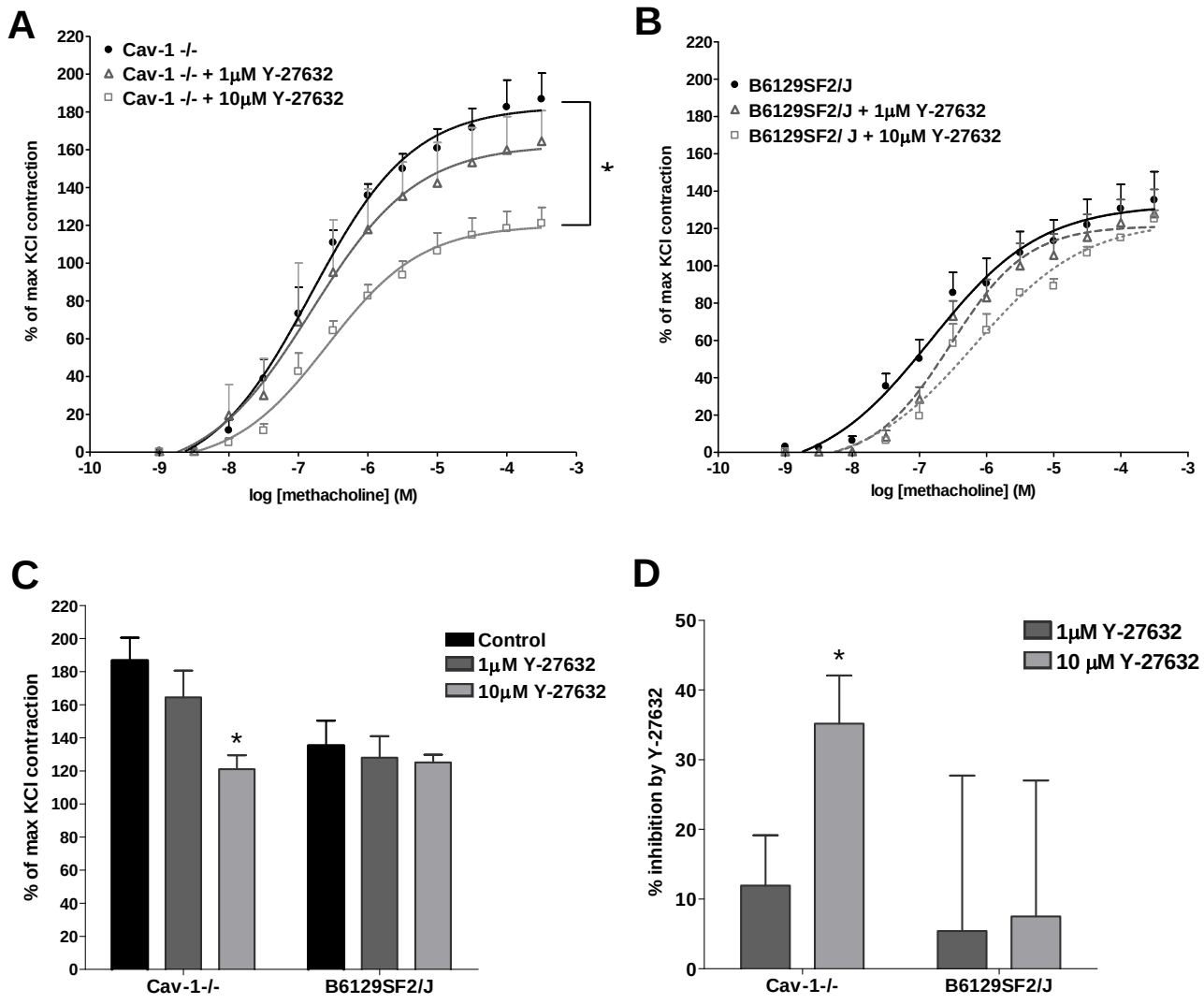

Figure 13: Effect of RhoA/Rho kinase (ROCK1/2) inhibition on methacholine induced tracheal smooth muscle contraction. (A) Comparison of methacholine induced contraction of tracheal ring preparations from caveolin-1 knockout (Cav-$1^{-/-}$) mice with and without administration of 1μM and 10 μM of known ROCK1/2 inhibitor – Y-27632. **(B)** Comparison of methacholine induced contraction of tracheal ring preparations from B6129SF2/J mice with and without administration of 1μM and 10 μM of known ROCK1/2 inhibitor Y-27632. **(C)** Comparison of responses to Y-27632 between mouse strains at maximum methacholine dose ($3x10^{-4}$ (3.5 on scale). Airway reactivity of tracheal smooth muscle from Cav-$1^{-/-}$ significantly decreased with administration of 10μM Y-27632 (*$p< 0.05$). Airway reactivity of tracheal smooth muscle from B6129SF2/J mice did not significantly differ with administration of Y-27632 ($p> 0.05$). Administration of 10μM Y-27632 normalized airway reactivity to methacholine between mouse strains. Tracheal smooth muscle preparations from Cav-$1^{-/-}$ mice remained hyperreactive compared with tracheal smooth muscle preparations from B6129SF2/J mice at baseline. **(D)** Comparison of the inhibition of tracheal smooth muscle contraction induced by administration of 1 μM and 10μM Y-27632. Values compared at maximum methacholine dose ($3x10^{-4}$). 10μM Y27632 was more effective at inhibiting airway smooth muscle responses in Cav-$1^{-/-}$ mice compared to B6129SF2/J mice (*$p<0.05$).

Following pretreatment with nebulized Y-27632 (5mM for 5min), methacholine-induced increases in central airway resistance (Rn), tissue damping (peripheral airway resistance) (G) and tissue elastance (H) were markedly reduced compared to baseline in both B6129SF2/J and Cav-$1^{-/-}$ mice. In fact, fully consistent with our *ex vivo* experiments, exposure to inhaled Y-27632 completely normalized both airway (Rn) and tissue (G) resistance between mouse strains (Figure 14).

Abundance of RhoA, ROCK 1, and ROCK 2 in lung and trachea tissue from Cav-$1^{-/-}$ mice

In order to determine whether the augmented contractile response in Cav-$1^{-/-}$ mice was associated with altered expression of some key signaling molecules of the RhoA/ROCK pathway, we assessed the protein abundance of RhoA, ROCK1 and ROCK2 in total lung and tracheal lysates from Cav-$1^{-/-}$ and B6129SF2/J mice. As shown in Figure 15, there was no significant differences in the expression of RhoA (Figure 15 A) and ROCK1 (Figure 15 B) in either tissue type between the mouse strains. Conversely, a small, but significant elevation in ROCK2 abundance was observed in the lungs and tracheas of Cav-$1^{-/-}$ mice compared with B6129SF2/J (Figure 15 C). This suggests ROCK2 signaling may be augmented in the absence of Cav-1 and may responsible for the airway hyperreactivity observed in Cav-$1^{-/-}$ mice. However, further studies are required to fully elucidate the signaling molecules/pathway responsible for the altered airway mechanics and enhanced airway smooth muscle contraction demonstrated in these animals.

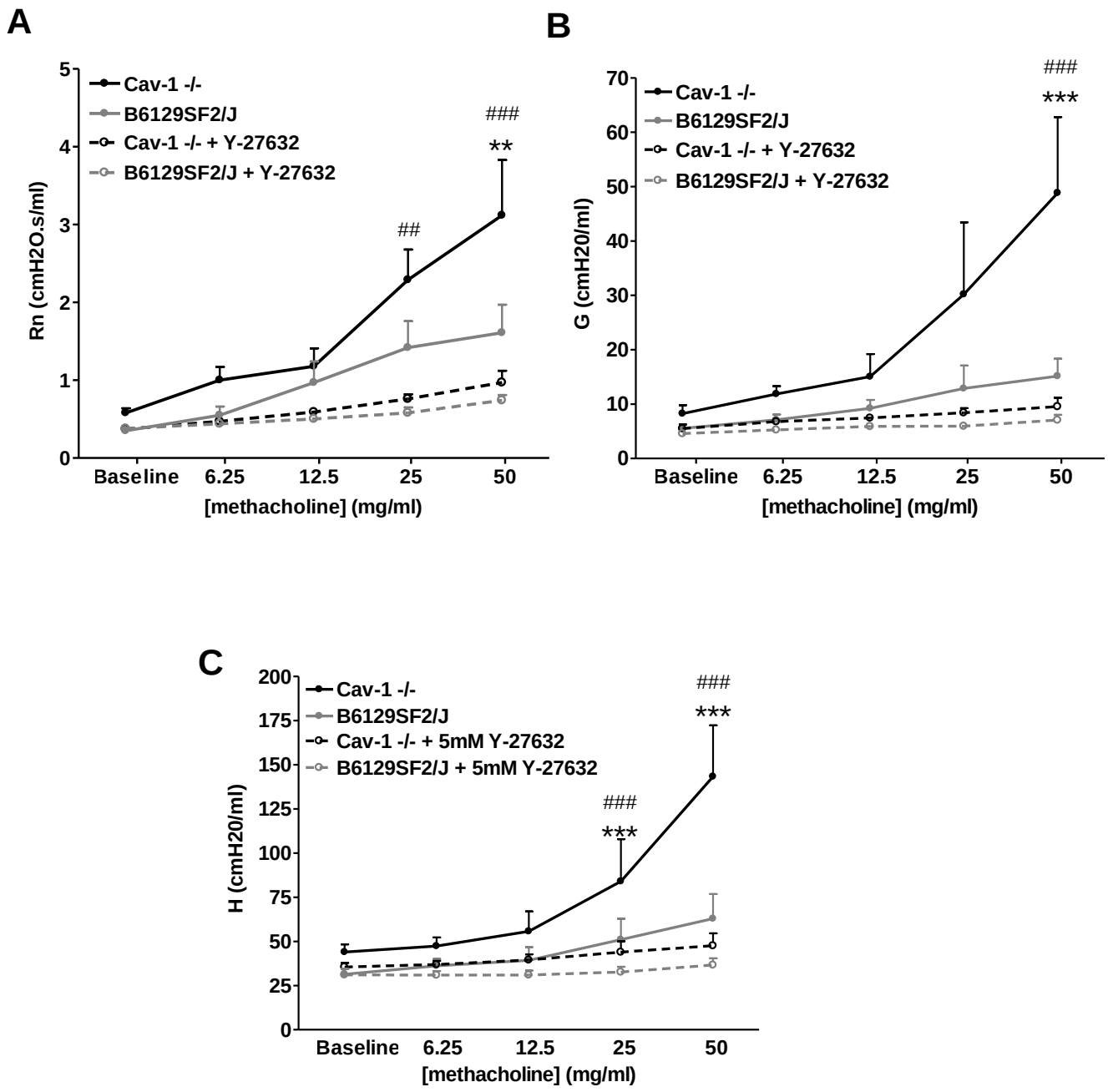

Figure 14- Respiratory mechanics of caveolin-1 knockout (Cav-1$^{-/-}$) and B6129SF2/J following inhalation of RhoA/Rho kinase (ROCK1/2) inhibitor, Y-27632. (A) Comparison of airway resistance (Rn) between Cav-1$^{-/-}$ and B6129SF2/J with increasing doses of inhaled methacholine, following inhalation of 5mM Y-27632. Cav-1$^{-/-}$ mice demonstrate significantly heightened airway resistance compared to B6129SF2/J mice at 50 mg/ml methacholine (** $p<0.01$). Following inhalation of Y-27632 there is a marked reduction in airway resistance in Cav-1$^{-/-}$ mice that reached significance at 25mg/ml ($^{##}p<0.01$) and 50 mg/ml methacholine ($^{###}p<0.001$). This reduction completely normalized responses between mouse strains at all doses of methacholine ($p>0.05$). There was no significant effect of Y-27632 inhalation on airway resistance in B6129SF2/J mice ($p>0.05$) **(B)** Comparison of tissue damping (G) between Cav-1$^{-/-}$ and B6129SF2/J with increasing doses of inhaled methacholine, following inhalation of 5mM Y-27632. Cav-1$^{-/-}$ mice demonstrate significantly heightened tissue damping compared to B6129SF2/J mice at 50 mg/ml methacholine (*** $p<0.001$). Following inhalation of Y-27632 there is a marked reduction in tissue damping

in Cav-1$^{-/-}$ mice that reached significance at 50 mg/ml methacholine ($^{###}$p<0.001). This reduction completely normalized responses between mouse strains at all doses of methacholine (p>0.05). There was no significant effect of Y-27632 inhalation on airway resistance in B6129SF2/J mice (p>0.05). **(C)** Comparison of tissue elastance (H) between Cav-1$^{-/-}$ and B6129SF2/J with increasing doses of inhaled methacholine, following inhalation of 5mM Y-27632. Cav-1$^{-/-}$ mice demonstrate significantly heightened tissue elastance compared to B6129SF2/J mice at 25mg/ml (***p<0.001) and 50 mg/ml methacholine (*** p<0.001). Following inhalation of Y-27632 there is a marked reduction in tissue elastance in Cav-1$^{-/-}$ mice that reached significance at 25mg/ml ($^{###}$p<0.001) and 50 mg/ml methacholine ($^{###}$p<0.001). This reduction completely normalized responses between mouse strains at all doses of methacholine (p>0.05). There was no significant effect of Y-27632 inhalation on airway resistance in B6129SF2/J mice (p>0.05).

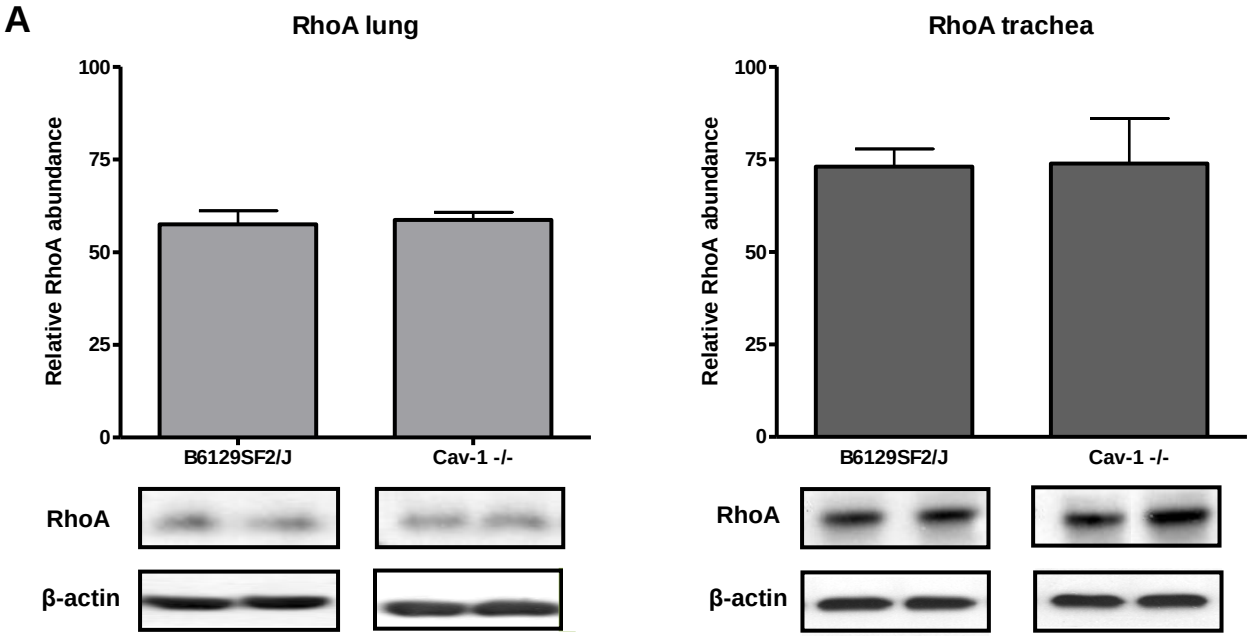

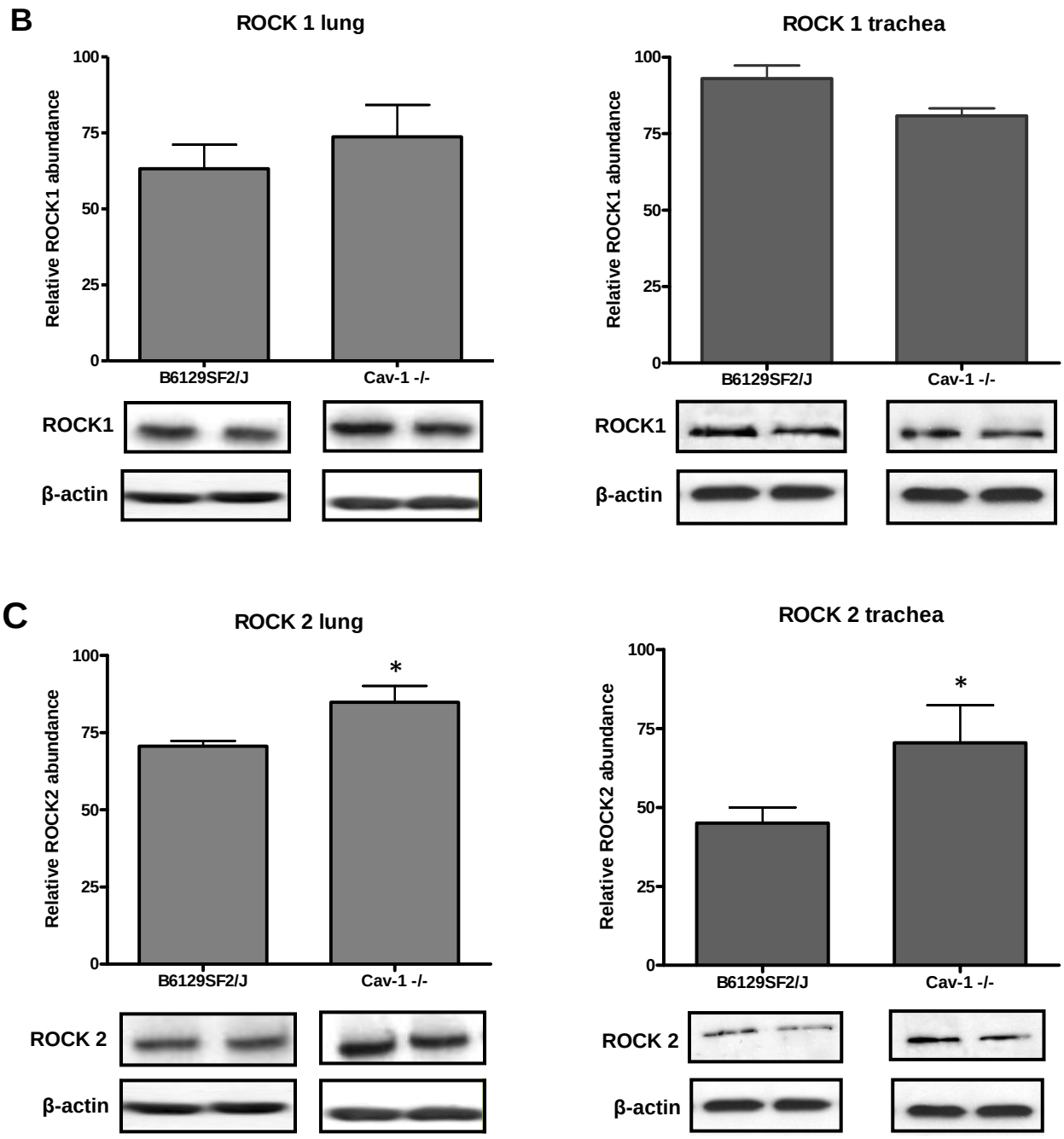

Figure 15: Abundance of RhoA (A), ROCK 1 (B), and ROCK 2 (C) protein expression in lung and tracheal tissue from caveolin-1 knockout (Cav-1$^{-/-}$) and B6129SF2/J mice. Representative blots for each protein and each tissue type is shown beneath each graph. There were no significant differences in RhoA **(A)** or ROCK 1 **(B)** protein expression between mouse strains in either lung or tracheal tissue. ROCK 2 **(C)** protein expression was significantly greater in both lung and trachea isolated from Cav-1$^{-/-}$ mice compared with B6129SF2/J mice (*$p<0.05$).

VII. Discussion

In this study we identify Cav-1 as a determinant of airway smooth muscle contraction, airway wall fibrosis, and respiratory mechanics. Previous studies have described an altered peripheral lung phenotype in Cav-$1^{-/-}$ mice characterized by thickened alveolar septae, reduced alveolar spaces and pulmonary fibrosis [30-32, 38]. The current study confirms and extends these observations as it provides a systematic assessment of the functional relevance of the altered organization of lung in Cav-$1^{-/-}$ mice, with particular focus on structural and functional changes of the airways. Cav-$1^{-/-}$ mice exhibit increased lung tissue elastance, indicating augmented stiffness that is consistent with the fibrotic and hypercellular nature of the peripheral lung. We also report that in response to supra-EC_{50} concentrations of inhaled methacholine, airway resistance and tissue resistance is elevated in Cav-$1^{-/-}$ mice. When studied *ex vivo*, tracheal smooth muscle from Cav-$1^{-/-}$ mice also displays hyperreactivity to methacholine, but sensitivity is not changed, suggesting that augmented airway smooth muscle contraction drives, in part, airway hyperreactivitiy *in vivo*. Cav-$1^{-/-}$ mice do not exhibit an increased abundance of airway smooth muscle, but are marked by increased airway wall collagen deposition. The accumulation of collagen we observed in Cav-$1^{-/-}$ mice suggests that structural remodeling of the airways also contributes to *in vivo* airway hyperreactivity. Furthermore, the enhanced fibrosis seen in the absence of Cav-1 produces a stiffening of the airways and parenchyma which increases overall lung elastance. Notably, in the BALF from naïve Cav-$1^{-/-}$, mice we observed a striking elevation of the pro-fibrotic cytokine TGF-β1, and of TNF-α, a multifunctional cytokine that has been linked to airway hyperresponsiveness. Thus, these cytokines may initiate and/or promote the development of the structural and functional alterations we observed in the airways of Cav-$1^{-/-}$ mice. Importantly, the changes in airway structure and function of Cav-$1^{-/-}$ mice occur in the

absence of inflammatory cell recruitment. This suggests a role for resident structural cells in cytokine release, for example, the epithelium is a rich source of pro-inflammatory and pro-fibrotic cytokines, including TGF-β1 and TNF-α [89-90]. Collectively, these experiments suggest that Cav-1 is an important regulator of the biological activity of airway cells that determines airway structure and function in health and disease.

To identify the pathway(s) involved in the augmented airway smooth muscle contractility observed in Cav-$1^{-/-}$ mice, we investigated 3 potential Ca^{2+} independent pathways that regulate smooth muscle contraction. We discovered that the inhibition of PKC and ERK1/2 pathways, with GF 109203X and U0126 respectively, did not affect the hyperreactivity to methacholine observed in tracheal preparations from Cav-$1^{-/-}$ mice and thus are not likely responsible. In contrast, inhibition of ROCK1/2 with Y-27632 completely reversed the hyperreactivity previously seen and produced comparable responses between mouse strains when challenged with methacholine both *in vivo* and *ex vivo*. Thus, we concluded that in the absence of Cav-1, augmented RhoA/Rho kinase (ROCK1/2) signaling was the likely source of smooth muscle hyperreactivity that contributed to the enhanced airway resistance observed *in vivo*. It is well documented that Cav-1 and RhoA interact upon receptor stimulation; however, the exact mechanism in which this interaction facilitates airway smooth muscle contraction is still unknown and will be the focus of our future studies [76-77].

This study quantitatively assessed differences in the structure of the airway walls of naive Cav-$1^{-/-}$ mice. Notably, significant accumulation of collagen developed in central and peripheral airways of Cav-$1^{-/-}$ mice. Structural remodeling of this nature is a hallmark feature of obstructive lung disease, and has been implicated in the development of fixed airway obstruction and hyperresponsiveness in asthma, as it likely underpins increased lumen narrowing during episodes

of airway smooth muscle spasm [9-10]. Thus, the accumulation of airway wall collagen that results from Cav-1 deficiency likely contributes, at least in part, to the central and peripheral airway hyperreactivity we measured in Cav-$1^{-/-}$ mice. The recent study by Le Saux is consistent with our findings [8]. They reported, in the absence of brochoconstrictor provocation, that airway resistance (Rn) and lung elastance (H) increased (and thus compliance decreased) as $Cav1^{-/-}$ mice aged. Our studies were performed with mice at an age (8-10 weeks) that preceded the measureable changes in $Cav1^{-/-}$ mouse respiratory mechanics; seen only after 12 weeks of age in the Le Saux study [8]. Our findings are consistent in that there were no differences in airway resistance, tissue damping and tissue elastance between Cav-$1^{-/-}$ and wild type mice at 8-10 weeks of age when challenged with saline. The differences in respiratory mechanics in our study were only evident once the mice were challenged with increasing doses of methacholine. Therefore, the augmented responses we demonstrated in Cav-$1^{-/-}$ mice likely reflect differences in fibroproliferative pathways and pathways controlling airway smooth muscle contraction that collectively contribute to enhanced airway narrowing in response to methacholine.

BALF from Cav-$1^{-/-}$ mice exhibited markedly elevated levels of the pro-fibrotic cytokine TGF-β1. This is consistent with a recent study that showed allergen exposure induced greater levels of TGFβ1 in the BALF from Cav-$1^{-/-}$ mice compared to C57BL/6 control mice [7]. Our findings are supported by a study which demonstrated that TGFβ1 blocking antibodies are sufficient to suppress the airway fibrosis that develops in mice after aerosol allergen challenge [91]. In human disease, lung tissue from patients with idiopathic pulmonary fibrosis exhibit reduced Cav-1 expression and this absence results in the TGF-β1-dependent activation of c-Jun N-terminal kinase (JNK) and accumulation of collagen and fibronectin [44]. *In vivo* studies with Cav-$1^{-/-}$ mice and *in vitro* studies using immortalized cell lines demonstrate at a cellular level that the loss

of Cav-1 is associated with augmented TGFβ type I receptor mediated activation of regulatory Smads; key transcription factors involved with collagen gene expression [7, 59]. Collectively, these studies demonstrate that the loss of Cav-1 appears to promote TGFβ1 release and permits the hyperactivation of TGFβ1-induced intracellular signaling pathways associated with collagen expression and release. Our results are completely consistent with these findings. The markedly increased levels of TGF-β1 we observed in BALF from Cav-1$^{-/-}$ mice likely initiate and promote the accumulation of collagen surrounding the airways that contribute to the airway fibrosis seen in these animals. Future studies to dissect the effects on TGFβ1 release and subsequent intracellular signaling responses may provide further insight into the airway remodeling process.

As airway smooth muscle is the key determinant of bronchoconstrictor responses, we quantified smooth muscle mass in central and peripheral airways of Cav-1$^{-/-}$ mice. Previous *in vitro* studies, including those from our own lab using human airway smooth muscle cells, revealed that the absence of Cav-1 promotes both spontaneous and mitogen-stimulated proliferation [5]. Despite these previous findings, in the current study, we did not detect any evidence for increased sm-α-actin staining in airways of naïve Cav-1$^{-/-}$ mice. Previous reports have similarly indicated that vascular smooth muscle abundance is not increased in untreated Cav-1$^{-/-}$ mice; however, excessive arterial myocyte proliferation leading to arterial stenosis develops in Cav-1$^{-/-}$ mice after balloon catheter injury [92]. This suggests that mitogenic stimulation is required before the absence of Cav-1 can drive smooth muscle mass accumulation. This is consistent with reports from us and others showing that endogenous Cav-1 is highest in quiescent airway and vascular smooth muscle cells and drops dramatically after mitogen exposure [5, 93]. Our experiments were restricted to naïve mice that had not been exposed to inhaled allergen, thus they retained an intact airway epithelium devoid of mucous containing goblet cells (data not shown), and showed

no evidence for the recruitment of inflammatory cells. However, a recent study from Le Saux et al shows that in mice subjected to allergen inhalation, an IL-4 dependent loss of caveolae and Cav-1 expression develops [7]. This suggests that the loss of Cav-1 in response to allergic inflammation could be associated with mesenchymal cell proliferative responses and subsequent changes in lung structure that characterize airway remodeling *in vivo*.

Our studies assessed airway inflammation and immune status in Cav-$1^{-/-}$ mice. ELISA of BALF supernatants showed that though both TNF-α and TGF-β1 were markedly increased, there was no change in the abundance of the stereotypical allergy-associated Th1 and Th2 cytokines, IFN-γ and IL-5, respectively. Moreover, we detected no change in the number or distribution of inflammatory cells in the airways of Cav-$1^{-/-}$ mice and serum immunoglobulin levels are comparable in both mouse strains. These data strongly suggest that the increased TNF-α and TGF-β1 in BALF from Cav-$1^{-/-}$ mice is not the result of idiopathic immune activation leading to airway recruitment of professional inflammatory cells. Instead, we believe these cytokines are likely derived from resident structural cells, such as the airway epithelium, fibroblasts and/or and airway smooth muscle. Expression of both TGF-β1 and TNF-α by epithelial and airway mesenchymal cells has been established previously [89-90]. Thus, our observations suggest that Cav-1 may be a central regulator of the pro-inflammatory and pro-fibrotic function of airway structural cells.

To directly assess the functional relevance of the structural changes in airways and peripheral lung that characterize Cav-$1^{-/-}$ mice, we measured respiratory mechanics from low frequency forced oscillation maneuvers using a small animal ventilator. Cav-$1^{-/-}$ mice demonstrated increased maximum lung elastance, and increased airway and tissue resistance, indicating that during inhaled methacholine exposure, structural changes correlate with greater stiffening of the

lung and hyperreactivity of the airways. The airway hyperreactivity we measured, which is marked by greater airway closure without a change in sensitivity to the bronchoconstricting agent, is consistent with the significant airway wall fibrosis present in Cav-$1^{-/-}$ mice. Thickening of the airway wall contributes to greater lumen closure without the need for altered contraction of the encircling airway smooth muscle. Nonetheless, our observations reveal significantly elevated levels of TNF-α in BALF from Cav-$1^{-/-}$ mice which suggests additional mechanisms could be at play. There is strong evidence that TNF-α contributes to airway hyperresponsiveness, as it is elevated in airways of human asthmatics, inhaled TNF-α induces and promotes airway hyperresponsiveness, and anti-TNF-α therapy can suppress airway hyperresponsiveness and improve lung function [90, 94-97]. TNF-α exposure also potentiates cholinergic agonist induced Ca^{2+} mobilization and contractile response of airway smooth muscle cells and isolated tissues [98]. Paradoxically, although our data shows airway hyperreactivity in Cav-$1^{-/-}$ mice, previous studies showed that Cav-1 expression is required for the contraction-potentiating effects of TNF-α on human airway smooth muscle cells [99]. Thus, future studies that measure the expression and localization of receptors for TNF-α and those that directly assess TNF-α induced signaling pathways in airway smooth muscle tissue from Cav-$1^{-/-}$ mice are highly warranted. Such studies will aim to determine the extent to which increased BALF TNF-α contributes directly to increased airway smooth muscle constriction triggered by inhaled methacholine.

To more directly assess whether altered airway smooth muscle contraction underpins the airway hyperreactivity observed in Cav-$1^{-/-}$ mice, we measured cumulative methacholine-induced contraction *ex vivo* using tracheal ring preparations. Tissue from Cav-$1^{-/-}$ mice exhibited increased reactivity as they generated significantly greater maximum force in response to supra-EC_{50} concentrations of methacholine. Notably, we saw no change in the sensitivity to

methacholine in Cav-1$^{-/-}$ mouse derived tracheal rings, as EC_{50} values were comparable to that measured for tissue from B6129SF2/J mice. Moreover, the abundance of airway smooth muscle and maximum contraction induced by KCl depolarization was not different between mouse strains. These data indicate that the maximum force of contraction induced by methacholine is increased in Cav-1$^{-/-}$ tissues. This highly is consistent with our *in vivo* observations showing heightened central and peripheral airway resistance at concentrations of inhaled methacholine which induce near-maximum or maximum loss of airway conductivity. Interestingly, the increase in airway smooth muscle contractility that occurs in the absence of Cav-1 cannot be accounted for by an increase in the amount of smooth muscle surrounding the airways. Thus, the heightened contraction is likely due to augmented Ca^{2+} dependent or independent intracellular signaling pathways that control airway smooth muscle contraction. Our *ex vivo* analyses of tracheal smooth muscle contractile responses are somewhat paradoxical in light of previous findings. Two studies, including one from our group, indicate that the acute depletion of caveolae or Cav-1 protein using cholesterol depleting agents or Cav-1 siRNA, suppresses both sensitivity to methacholine (but not maximum intracellular Ca^{2+} mobilization) and contraction of isolated canine or human airway smooth muscle [6, 45]. However, these studies differ significantly from the *ex vivo* analyses we performed in the current study as the depletion of caveolae and Cav-1 was acute in these studies and likely had little effect on expression of other genes. In addition, in the previous studies, the effects of excess collagen deposition were avoided and tissues were not subjected to prolonged exposure to elevated levels of TGFβ1 and TNF-α, as is the case for airway smooth muscle from Cav-1$^{-/-}$ mice. Furthermore, it is possible that Cav-1 participates in different regulatory roles in both Ca^{2+} dependent (Figure 2) and Ca^{2+} independent (Figure 3) pathways of smooth muscle contraction. The effects seen on Ca^{2+} mobilization in our

previous studies may reflect the role Cav-1 has in regulating Ca^{2+} dependent pathways; whereas the effects seen in the current study appear to involve regulation of Ca^{2+} independent pathways; most notably, RhoA/ROCK1/2 signaling.

We discovered that enhanced RhoA/ROCK1/2 signaling was the likely cause of the augmented smooth muscle contractility and airway hyperreactivity observed in Cav $-1^{-/-}$ mice. It is well recognized that Cav-1 directly interacts with and regulates both PKC and RhoA/ROCK1/2 signaling to alter smooth muscle contractility [37, 67, 77-78]. Interestingly, we found no change in the methacholine induced tracheal smooth muscle contractility with inhibition of PKC signaling in either mouse strain, suggesting little participation from this pathway in augmenting airway smooth muscle contractility in this study. Conversely, inhibition of ROCK1/2 significantly reduced tracheal smooth muscle contractility in Cav-$1^{-/-}$ mice to levels that were comparable to B6129SF2/J mice. Similarly, inhalation of Y-27632 completely eliminated differences in central airway resistance (Rn) and tissue resistance (G) between mouse stains in our *in vivo* studies. As stated previously, RhoA and Rho kinase (ROCK1/2) are known to mediate Ca^{2+} independent regulation of sustained and maximum force generation and have previously been shown to associate with and be inhibited by Cav-1 [37, 76-77]. These studies show that agonist induced activation of RhoA can be inhibited by cell permeable peptides that mimic the caveolin scaffolding domain, and results in reduced contraction of isolated arterial myocytes [76-77]. Moreover, a recent study highly consistent with our findings showed that RhoA activity is elevated and contractility is enhanced in gastrointestinal smooth muscle from Cav-$1^{-/-}$ mice [37, 67]. Additional studies show paradoxical results which further obfuscate the exact role of Cav-1 in regulating smooth muscle contraction. Somara et al demonstrated that aged colonic smooth muscle with reduced motility has reduced expression of Cav-1 and ectopic

expression of Cav-1 restored contractile responses through the activation of RhoA/ROCK1/2 signaling [67]. An additional study by Dubroca et al demonstrated that myogenic tone in the mesenteric arteries of rats was reduced by inhibition of Cav-1, disruption of caveolae and inhibition of RhoA indicating the interaction between Cav-1 and RhoA is not inhibitory but may be activating instead [78]. Unfortunately, the interaction between Cav-1 and RhoA/ROCK1/2 signaling has yet to be explored in airway smooth muscle and thus the interactions described above may or may not be specific to the muscle type studied. In addition, most of the studies induced the inhibition of Cav-1/disruption of caveolae in an acute fashion and thus these interactions may be significantly different in Cav-$1^{-/-}$ mice who have been Cav-1 deficient for their entire life. Furthermore, our studies do not provide direct insight into excitation contraction coupling in airway smooth muscle from Cav-$1^{-/-}$ mice, as we did not measure intracellular Ca^{2+} mobilization or the activity of Ca^{2+} independent pro-contractile pathways. It appears as though ROCK 2 expression is elevated in Cav-$1^{-/-}$ mice and thus may be the source for the enhanced contractility; however, further studies measuring activity of each of these signaling molecules is required before any concrete conclusions can be made. Thus, based on our current findings and the paucity of evidence regarding the exact role of these pathways in airway smooth muscle, it is clear that these issues require a more in depth analysis. Experiments using lung slice preparations, as well as pharmacological and molecular interventions for gain- and loss-of-function studies are highly warranted. Such studies will help to dissect the mechanisms intrinsic to contractile airway smooth muscle that contribute to the enhanced airway smooth muscle contractility and the airway hyperreactivity observed in in Cav-$1^{-/-}$ mice.

Thus in summary, in response to inhaled methacholine, naive Cav-$1^{-/-}$ mice exhibit altered respiratory mechanics, including increased maximum lung elastance, tissue resistance and airway

resistance. These functional alterations correlate with structural changes in the lung, including alveolar thickening and fibrosis of the central and peripheral airways. Brochoalveolar fluid from Cav-$1^{-/-}$ mice exhibits increased levels of TGF-β1 and TNF-α, which are likely secreted by resident structural cells, as inflammatory cell number is similar to control mouse strains. Moreover, we show that serum immunoglobin levels and innate immune responses are unaffected by Cav-1 deficiency. Increased TGFβ1 and TNF-α in BALF are likely linked to airway wall fibrosis and airway hyperreactivity, though the precise mechanisms for these effects require further study. Airway hyperreactivity in Cav-$1^{-/-}$ mice correlates with augmented contractile reactivity of isolated tracheal smooth muscle from Cav-$1^{-/-}$ mice; thus, altered airway smooth muscle contraction and structural remodeling of the central and peripheral airways appear to work in concert to underpin *in vivo* airway hyperreactivity. Furthermore, it appears that the chronic absence of Cav-1 leads to enhanced RhoA/ROCK1/2 signaling that potentiate this hyperreactivity; suggesting that when present, Cav-1 plays an inhibitory role on this pathway. However, further studies are required to fully elucidate these interactions, as well as investigate the role Cav-1 has on Ca^{2+} dependent pathways of airway smooth muscle contraction. While the role of Cav-1 in the pathophysiology of asthma and airway remodeling is still under investigation, a recent report provided new insight. Le Saux et al demonstrated that acute allergen exposure leads airway remodeling and reduced Cav-1 expression in the mouse lung thus suggesting that Cav-1 serves a protective role against the changes that occur in the airways in allergic asthma [7]. Our results are therefore important as they further support a probable role for Cav-1 in the airway remodeling as well as the intrinsic changes to airway smooth muscle that develop and contribute to human allergic asthma.

VIII. References

1. The National Asthma Control Task Force, *The prevention and management of asthma in Canada: a major challenge now and in the future*. 2000.

2. Gosens, R., et al., *Caveolae and caveolins in the respiratory system.* Curr Mol Med, 2008. **8**(8): p. 741-53.

3. R Gosens, G.S., ST Bos, G Dueck, MM Mutawe, D Schaafsma, H Unruh, WT Gerthoffer, J Zaagsma, H Meurs & AJ Halayko, *Caveolin-1 is required for contractile phenotype maturation by airway smooth muscle cells.* J Cell Mol Med, 2010.

4. Halayko, A.J., T. Tran, and R. Gosens, *Phenotype and functional plasticity of airway smooth muscle: role of caveolae and caveolins.* Proc Am Thorac Soc, 2008. **5**(1): p. 80-8.

5. Gosens, R., Stelmack, G. L., Dueck, G., McNeill, K. D., Yamasaki, A., Gerthoffer, W. T., Unruh, H., Gounni, A. S., Zaagsma, J., Halayko, A. J., *Role of caveolin-1 in p42/p44 MAP kinase activation and proliferation of human airway smooth muscle.* Am J Physiol Lung Cell Mol Physiol, 2006. **291**(3): p. L523-34.

6. Gosens, R., Stelmack, G. L., Dueck, G., Mutawe, M. M., Hinton, M. A., McNeill, K. D., Paulson, A., Dakshinamurti, S., Gerthoffer, W. T., Thliveris, J. A., Unruh, H., Zaagsma, J., Halayko, A. J., *Caveolae Facilitate Muscarinic Receptor Mediated Intracellular Ca2+ Mobilization and Contraction in Airway Smooth Muscle.* Am J Physiol Lung Cell Mol Physiol, 2007.

7. Jourdan Le Saux, C.T., Teeters, K. M., Miyasato, S. K., Hoffmann, P. R., Bollt, O. M., Douet, V., Shohet, R. V., Broide, D. H., Tam, E. K., *Down-regulation of caveolin-1, an inhibitor of TGF-beta signaling, in acute allergen-induced airway remodeling.* J Biol Chem, 2007.

8. Le Saux, O., et al., *The role of caveolin-1 in pulmonary matrix remodeling and mechanical properties.* Am J Physiol Lung Cell Mol Physiol, 2008. **295**(6): p. L1007-17.

9. Holgate, S.T., *Pathogenesis of asthma.* Clin Exp Allergy, 2008. **38**(6): p. 872-97.

10. Bai, T.R. and D.A. Knight, *Structural changes in the airways in asthma: observations and consequences.* Clin Sci (Lond), 2005. **108**(6): p. 463-77.

11. Epstein, M.M., *Do mouse models of allergic asthma mimic clinical disease?* Int Arch Allergy Immunol, 2004. **133**(1): p. 84-100.

12. Busse, W.W. and R.F. Lemanske, Jr., *Asthma.* N Engl J Med, 2001. **344**(5): p. 350-62.

13. Holgate, S.T., et al., *A new look at the pathogenesis of asthma.* Clin Sci (Lond). **118**(7): p. 439-50.

14. Jackson, D.J., et al., *Wheezing rhinovirus illnesses in early life predict asthma development in high-risk children.* Am J Respir Crit Care Med, 2008. **178**(7): p. 667-72.

15. Whitehead, G.S., et al., *Allergen-induced airway disease is mouse strain dependent.* Am J Physiol Lung Cell Mol Physiol, 2003. **285**(1): p. L32-42.

16. Barbato, A., et al., *Epithelial damage and angiogenesis in the airways of children with asthma.* Am J Respir Crit Care Med, 2006. **174**(9): p. 975-81.

17. Fedorov, I.A., et al., *Epithelial stress and structural remodelling in childhood asthma.* Thorax, 2005. **60**(5): p. 389-94.

18. Holgate, S.T., et al., *Epithelial-mesenchymal communication in the pathogenesis of chronic asthma.* Proc Am Thorac Soc, 2004. **1**(2): p. 93-8.

19. Bai, T.R., *Evidence for airway remodeling in chronic asthma.* Curr Opin Allergy Clin Immunol. **10**(1): p. 82-6.

20. Warner, S.M. and D.A. Knight, *Airway modeling and remodeling in the pathogenesis of asthma.* Curr Opin Allergy Clin Immunol, 2008. **8**(1): p. 44-8.

21. Puddicombe, S.M., et al., *Increased expression of p21(waf) cyclin-dependent kinase inhibitor in asthmatic bronchial epithelium.* Am J Respir Cell Mol Biol, 2003. **28**(1): p. 61-8.

22. Kicic, A., et al., *Intrinsic biochemical and functional differences in bronchial epithelial cells of children with asthma.* Am J Respir Crit Care Med, 2006. **174**(10): p. 1110-8.

23. James, A.L., et al., *Airway smooth muscle thickness in asthma is related to severity but not duration of asthma.* Eur Respir J, 2009. **34**(5): p. 1040-5.

24. Palade, G., *Fine Structure of Blood Capillaries.* J. Appl. Physiol., 1953. **24**: p. 1424-1436.

25. Yamada, E., *The fine structure of the gall bladder epithelium of the mouse.* J Biophys Biochem Cytol, 1955. **1**(5): p. 445-58.

26. Fujimoto, T., et al., *Caveolae: from a morphological point of view.* J Electron Microsc (Tokyo), 1998. **47**(5): p. 451-60.

27. Smart, E.J., et al., *Caveolins, liquid-ordered domains, and signal transduction.* Mol Cell Biol, 1999. **19**(11): p. 7289-304.

28. Williams, T.M. and M.P. Lisanti, *The Caveolin genes: from cell biology to medicine.* Ann Med, 2004. **36**(8): p. 584-95.

29. Cohen, A.W., et al., *Role of caveolae and caveolins in health and disease.* Physiol Rev, 2004. **84**(4): p. 1341-79.

30. Hnasko, R., Lisanti, M. P., *The biology of caveolae: lessons from caveolin knockout mice and implications for human disease.* Mol Interv, 2003. **3**(8): p. 445-64.

31. Razani, B., Lisanti, M. P., *Caveolin-deficient mice: insights into caveolar function human disease.* J Clin Invest, 2001. **108**(11): p. 1553-61.

32. Drab, M., Verkade, P., Elger, M., Kasper, M., Lohn, M., Lauterbach, B., Menne, J., Lindschau, C., Mende, F., Luft, F. C., Schedl, A., Haller, H., Kurzchalia, T. V., *Loss of caveolae, vascular dysfunction, and pulmonary defects in caveolin-1 gene-disrupted mice.* Science, 2001. **293**(5539): p. 2449-52.

33. Galbiati, F., Volonte, D., Liu, J., Capozza, F., Frank, P. G., Zhu, L., Pestell, R. G., Lisanti, M. P., *Caveolin-1 expression negatively regulates cell cycle progression by inducing G(0)/G(1) arrest via a p53/p21(WAF1/Cip1)-dependent mechanism.* Mol Biol Cell, 2001. **12**(8): p. 2229-44.

34. Glenney, J.R., Jr., *Tyrosine phosphorylation of a 22-kDa protein is correlated with transformation by Rous sarcoma virus.* J Biol Chem, 1989. **264**(34): p. 20163-6.

35. Glenney, J.R., Jr. and D. Soppet, *Sequence and expression of caveolin, a protein component of caveolae plasma membrane domains phosphorylated on tyrosine in Rous sarcoma virus-transformed fibroblasts.* Proc Natl Acad Sci U S A, 1992. **89**(21): p. 10517-21.

36. Tang, Z., et al., *Molecular cloning of caveolin-3, a novel member of the caveolin gene family expressed predominantly in muscle.* J Biol Chem, 1996. **271**(4): p. 2255-61.

37. Shakirova, Y., Bonnevier, J., Albinsson, S., Adner, M., Rippe, B., Broman, J.m, Arner, A., Sward, K., *Increased Rho activation and PKC-mediated smooth muscle contractility in the absence of caveolin-1.* Am J Physiol Cell Physiol, 2006. **291**(6): p. C1326-35.

38. Razani, B., Engelman, J. A., Wang, X. B., Schubert, W., Zhang, X. L., Marks, C. B., Macaluso, F., Russell, R. G., Li, M., Pestell, R. G., Di Vizio, D., Hou, H., Jr., Kneitz, B., Lagaud, G., Christ, G. J., Edelmann, W., Lisanti, M. P., *Caveolin-1 null mice are viable but show evidence of hyperproliferative and vascular abnormalities.* J Biol Chem, 2001. **276**(41): p. 38121-38.

39. Razani, B., S.E. Woodman, and M.P. Lisanti, *Caveolae: from cell biology to animal physiology.* Pharmacol Rev, 2002. **54**(3): p. 431-67.

40. Garcia-Cardena, G., et al., *Dissecting the interaction between nitric oxide synthase (NOS) and caveolin. Functional significance of the nos caveolin binding domain in vivo.* J Biol Chem, 1997. **272**(41): p. 25437-40.

41. Ghosh, S., et al., *Interaction between caveolin-1 and the reductase domain of endothelial nitric-oxide synthase. Consequences for catalysis.* J Biol Chem, 1998. **273**(35): p. 22267-71.

42. Michel, J.B., et al., *Reciprocal regulation of endothelial nitric-oxide synthase by Ca2+-calmodulin and caveolin.* J Biol Chem, 1997. **272**(25): p. 15583-6.

43. Wang, X.M., Kim, H. P., Song, R., Choi, A. M., *Caveolin-1 confers antiinflammatory effects in murine macrophages via the MKK3/p38 MAPK pathway.* Am J Respir Cell Mol Biol, 2006. **34**(4): p. 434-42.

44. Wang, X.M., Zhang, Y., Kim, H. P., Zhou, Z., Feghali-Bostwick, C. A., Liu, F., Ifedigbo, E., Xu, X., Oury, T. D.. Kaminski, N., Choi, A. M., *Caveolin-1: a critical regulator of lung fibrosis in idiopathic pulmonary fibrosis.* J Exp Med, 2006. **203**(13): p. 2895-906.

45. Prakash, Y.S., Thompson, M. A., Vaa, B., Matabdin, I., Peterson, T. E., He, T., Pabelick, C. M., *Caveolins and Intracellular Calcium Regulation in Human Airway Smooth Muscle.* Am J Physiol Lung Cell Mol Physiol, 2007.

46. Dreja, K., et al., *Cholesterol depletion disrupts caveolae and differentially impairs agonist-induced arterial contraction.* Arterioscler Thromb Vasc Biol, 2002. **22**(8): p. 1267-72.

47. Galbiati, F., B. Razani, and M.P. Lisanti, *Emerging themes in lipid rafts and caveolae.* Cell, 2001. **106**(4): p. 403-11.

48. Park, D.S., Cohen, A. W., Frank, P. G., Razani, B., Lee, H., Williams, T. M., Chandra, M., Shirani, J., De Souza, A. P., Tang, B., Jelicks, L. A., Factor, S. M., Weiss, L. M., Tanowitz, H. B., Lisanti, M. P., *Caveolin-1 null (-/-) mice show dramatic reductions in life span.* Biochemistry, 2003. **42**(51): p. 15124-31.

49. Halayko, A.J. and G.L. Stelmack, *The association of caveolae, actin, and the dystrophin-glycoprotein complex: a role in smooth muscle phenotype and function?* Can J Physiol Pharmacol, 2005. **83**(10): p. 877-91.

50. Bergdahl, A. and K. Sward, *Caveolae-associated signalling in smooth muscle.* Can J Physiol Pharmacol, 2004. **82**(5): p. 289-99.

51. Kim, H.P., Choi, A. M., *Caveolin-1 stops profibrogenic signaling?* Am J Physiol Lung Cell Mol Physiol, 2008. **294**(5): p. L841-2.

52. Fernandes, D.J., Bonacci, J. V., Stewart, A. G., *Extracellular matrix, integrins, and mesenchymal cell function in the airways.* Curr Drug Targets, 2006. **7**(5): p. 567-77.

53. Halayko, A.J., Tran, T., Ji, S. Y., Yamasaki, A., Gosens, R., *Airway smooth muscle phenotype and function: interactions with current asthma therapies.* Curr Drug Targets, 2006. **7**(5): p. 525-40.

54. Hirst, S.J., Martin, J. G., Bonacci, J. V., Chan, V., Fixman, E. D., Hamid, Q. A., Herszberg, B., Lavoie, J. P., McVicker, C. G., Moir, L. M., Nguyen, T. T., Peng, Q., Ramos-Barbon, D., Stewart, A. G., *Proliferative aspects of airway smooth muscle.* J Allergy Clin Immunol, 2004. **114**(2 Suppl): p. S2-17.

55. Postma, D.S., Timens, W., *Remodeling in asthma and chronic obstructive pulmonary disease.* Proc Am Thorac Soc, 2006. **3**(5): p. 434-9.

56. Selman, M., Thannickal, V. J., Pardo, A., Zisman, D. A., Martinez, F. J., Lynch, J. P., 3rd, *Idiopathic pulmonary fibrosis: pathogenesis and therapeutic approaches.* Drugs, 2004. **64**(4): p. 405-30.

57. Verma, S., Slutsky, A. S., *Idiopathic pulmonary fibrosis--new insights.* N Engl J Med, 2007. **356**(13): p. 1370-2.

58. Lee, E.K., Lee, Y. S., Han, I. O., Park, S. H., *Expression of Caveolin-1 reduces cellular responses to TGF-beta1 through down-regulating the expression of TGF-beta type II receptor gene in NIH3T3 fibroblast cells.* Biochem Biophys Res Commun, 2007. **359**(2): p. 385-90.

59. Razani, B., Zhang, X. L., Bitzer, M., von Gersdorff, G., Bottinger, E. P., Lisanti, M. P., *Caveolin-1 regulates transforming growth factor (TGF)-beta/SMAD signaling through an interaction with the TGF-beta type I receptor.* J Biol Chem, 2001. **276**(9): p. 6727-38.

60. Galbiati, F., Volonte, D., Engelman, J. A., Watanabe, G., Burk, R., Pestell, R. G., Lisanti, M. P., *Targeted downregulation of caveolin-1 is sufficient to drive cell transformation and hyperactivate the p42/44 MAP kinase cascade.* Embo J, 1998. **17**(22): p. 6633-48.

61. Volonte, D., Zhang, K., Lisanti, M. P., Galbiati, F., *Expression of caveolin-1 induces premature cellular senescence in primary cultures of murine fibroblasts.* Mol Biol Cell, 2002. **13**(7): p. 2502-17.

62. Rayment, I., et al., *Three-dimensional structure of myosin subfragment-1: a molecular motor.* Science, 1993. **261**(5117): p. 50-8.

63. Harada, Y., et al., *Sliding movement of single actin filaments on one-headed myosin filaments.* Nature, 1987. **326**(6115): p. 805-8.

64. Kron, S.J. and J.A. Spudich, *Fluorescent actin filaments move on myosin fixed to a glass surface.* Proc Natl Acad Sci U S A, 1986. **83**(17): p. 6272-6.

65. Stephens, N.L., et al., *The contractile apparatus of airway smooth muscle. Biophysics and biochemistry.* Am J Respir Crit Care Med, 1998. **158**(5 Pt 3): p. S80-94.

66. Stephens, N.L., *Airway smooth muscle.* Lung, 2001. **179**(6): p. 333-73.

67. Somara, S., Gilmont, R. R., Martens, J. R., Bitar, K. N., *Ectopic expression of caveolin-1 restores physiological contractile response of aged colonic smooth muscle.* Am J Physiol Gastrointest Liver Physiol, 2007. **293**(1): p. G240-9.

68. Pfitzer, G., *Invited review: regulation of myosin phosphorylation in smooth muscle.* J Appl Physiol, 2001. **91**(1): p. 497-503.

69. Schaafsma, D., Gosens, R., Zaagsma, J., Halayko, A. J., Meurs, H., *Rho kinase inhibitors: a novel therapeutical intervention in asthma?* Eur J Pharmacol, 2008. **585**(2-3): p. 398-406.

70. Webb, R.C., *Smooth muscle contraction and relaxation.* Adv Physiol Educ, 2003. **27**(1-4): p. 201-6.

71. Somlyo, A.P., Somlyo, A. V., *Signal transduction by G-proteins, rho-kinase and protein phosphatase to smooth muscle and non-muscle myosin II.* J Physiol, 2000. **522 Pt 2**: p. 177-85.

72. Murray, R.K., Kotlikoff, M. I., *Receptor-activated calcium influx in human airway smooth muscle cells.* J Physiol, 1991. **435**: p. 123-44.

73. Worley, J.F., 3rd, Kotlikoff, M. I., *Dihydropyridine-sensitive single calcium channels in airway smooth muscle cells.* Am J Physiol, 1990. **259**(6 Pt 1): p. L468-80.

74. Lohn, M., Furstenau, M., Sagach, V., Elger, M., Schulze, W., Luft, F. C., Haller, H., Gollasch, M., *Ignition of calcium sparks in arterial and cardiac muscle through caveolae.* Circ Res, 2000. **87**(11): p. 1034-9.

75. Sanders, K.M., *Invited review: mechanisms of calcium handling in smooth muscles.* J Appl Physiol, 2001. **91**(3): p. 1438-49.

76. Gingras, D., Gauthier, F., Lamy, S., Desrosiers, R. R., Beliveau, R., *Localization of RhoA GTPase to endothelial caveolae-enriched membrane domains.* Biochem Biophys Res Commun, 1998. **247**(3): p. 888-93.

77. Taggart, M.J., Leavis, P., Feron, O., Morgan, K. G., *Inhibition of PKCalpha and rhoA translocation in differentiated smooth muscle by a caveolin scaffolding domain peptide.* Exp Cell Res, 2000. **258**(1): p. 72-81.

78. Dubroca, C., Loyer, X., Retailleau, K., Loirand, G., Pacaud, P., Feron, O., Balligand, J. L., Levy, B. I., Heymes, C., Henrion, D., *RhoA activation and interaction with Caveolin-1 are critical for pressure-induced myogenic tone in rat mesenteric resistance arteries.* Cardiovasc Res, 2007. **73**(1): p. 190-7.

79. Garrean, S., Gao, X. P., Brovkovych, V., Shimizu, J., Zhao, Y. Y., Vogel, S. M., Malik, A. B., *Caveolin-1 regulates NF-kappaB activation and lung inflammatory response to sepsis induced by lipopolysaccharide.* J Immunol, 2006. **177**(7): p. 4853-60.

80. Bucci, M., Gratton, J. P., Rudic, R. D., Acevedo, L., Roviezzo, F., Cirino, G., Sessa, W. C., *In vivo delivery of the caveolin-1 scaffolding domain inhibits nitric oxide synthesis and reduces inflammation.* Nat Med, 2000. **6**(12): p. 1362-7.

81. Schaafsma, D., Bos, I. S., Zuidhof, A. B., Zaagsma, J., Meurs, H., *Inhalation of the Rho-kinase inhibitor Y-27632 reverses allergen-induced airway hyperresponsiveness after the early and late asthmatic reaction.* Respir Res, 2006. **7**: p. 121.

82. Hirota, J.A., Ellis, R., Inman, M. D., *Regional differences in the pattern of airway remodeling following chronic allergen exposure in mice.* Respir Res, 2006. **7**(1): p. 120.

83. Gordon, J.R., Li, F., Nayyar, A., Xiang, J., Zhang, X., *CD8 alpha+, but not CD8 alpha-, dendritic cells tolerize Th2 responses via contact-dependent and -independent mechanisms, and reverse airway hyperresponsiveness, Th2, and eosinophil responses in a mouse model of asthma.* J Immunol, 2005. **175**(3): p. 1516-22.

84. Schneider, A.M., Li, F., Zhang, X., Gordon, J. R., *Induction of pulmonary allergen-specific IgA responses or airway hyperresponsiveness in the absence of allergic lung disease following sensitization with limiting doses of ovalbumin-alum.* Cell Immunol, 2001. **212**(2): p. 101-9.

85. Adner, M., Rose, A. C., Zhang, Y., Sward, K., Benson, M., Uddman, R., Shankley, N. P., Cardell, L. O., *An assay to evaluate the long-term effects of inflammatory mediators on murine airway smooth muscle: evidence that TNFalpha up-regulates 5-HT(2A)-mediated contraction.* Br J Pharmacol, 2002. **137**(7): p. 971-82.

86. Chiba, Y., Yanagisawa, R., Sagai, M., *Strain and route differences in airway responsiveness to acetylcholine in mice.* Res Commun Mol Pathol Pharmacol, 1995. **90**(1): p. 169-72.

87. Takeda, K., Haczku, A., Lee, J. J., Irvin, C. G., Gelfand, E. W., *Strain dependence of airway hyperresponsiveness reflects differences in eosinophil localization in the lung.* Am J Physiol Lung Cell Mol Physiol, 2001. **281**(2): p. L394-402.

88. Duguet, A., Biyah, K., Minshall, E., Gomes, R., Wang, C. G., Taoudi-Benchekroun, M., Bates, J. H., Eidelman, D. H., *Bronchial responsiveness among inbred mouse strains. Role of airway smooth-muscle shortening velocity.* Am J Respir Crit Care Med, 2000. **161**(3 Pt 1): p. 839-48.

89. Thomas, P.S., *Tumour necrosis factor-alpha: the role of this multifunctional cytokine in asthma.* Immunol Cell Biol, 2001. **79**(2): p. 132-40.

90. Howarth, P.H., Babu, K. S., Arshad, H. S., Lau, L., Buckley, M., McConnell, W., Beckett, P., Al Ali, M., Chauhan, A., Wilson, S. J., Reynolds, A., Davies, D. E., Holgate, S. T., *Tumour necrosis factor (TNFalpha) as a novel therapeutic target in symptomatic corticosteroid dependent asthma.* Thorax, 2005. **60**(12): p. 1012-8.

91. Alcorn, J.F., et al., *Transforming growth factor-beta1 suppresses airway hyperresponsiveness in allergic airway disease.* Am J Respir Crit Care Med, 2007. **176**(10): p. 974-82.

92. Hassan, G.S., Jasmin, J. F., Schubert, W., Frank, P. G., Lisanti, M. P., *Caveolin-1 deficiency stimulates neointima formation during vascular injury.* Biochemistry, 2004. **43**(26): p. 8312-21.

93. Peterson, T.E., Guicciardi, M. E., Gulati, R., Kleppe, L. S., Mueske, C. S., Mookadam, M., Sowa, G., Gores, G. J., Sessa, W. C., Simari, R. D., *Caveolin-1 can regulate vascular smooth muscle cell fate by switching platelet-derived growth factor signaling from a proliferative to an apoptotic pathway.* Arterioscler Thromb Vasc Biol, 2003. **23**(9): p. 1521-7.

94. Thomas, P.S., Heywood, G., *Effects of inhaled tumour necrosis factor alpha in subjects with mild asthma.* Thorax, 2002. **57**(9): p. 774-8.

95. Thomas, P.S., Yates, D. H., Barnes, P. J., *Tumor necrosis factor-alpha increases airway responsiveness and sputum neutrophilia in normal human subjects.* Am J Respir Crit Care Med, 1995. **152**(1): p. 76-80.

96. Berry, M., Brightling, C., Pavord, I., Wardlaw, A., *TNF-alpha in asthma.* Curr Opin Pharmacol, 2007. **7**(3): p. 279-82.

97. Berry, M.A., Hargadon, B., Shelley, M., Parker, D., Shaw, D. E., Green, R. H., Bradding, P., Brightling, C. E., Wardlaw, A. J., Pavord, I. D., *Evidence of a role of tumor necrosis factor alpha in refractory asthma.* N Engl J Med, 2006. **354**(7): p. 697-708.

98. Chen, H., Tliba, O., Van Besien, C. R., Panettieri, R. A., Jr., Amrani, Y., *TNF-[alpha] modulates murine tracheal rings responsiveness to G-protein-coupled receptor agonists and KCl.* J Appl Physiol, 2003. **95**(2): p. 864-72; discussion 863.

99. Hunter, I., Nixon, G. F., *Spatial compartmentalization of tumor necrosis factor (TNF) receptor 1-dependent signaling pathways in human airway smooth muscle cells. Lipid rafts are essential for TNF-alpha-mediated activation of RhoA but dispensable for the activation of the NF-kappaB and MAPK pathways.* J Biol Chem, 2006. **281**(45): p. 34705-15.